

Swarm dynamics and equilibria for a nonlocal aggregation model

This content has been downloaded from IOPscience. Please scroll down to see the full text.

2011 Nonlinearity 24 2681

(<http://iopscience.iop.org/0951-7715/24/10/002>)

View [the table of contents for this issue](#), or go to the [journal homepage](#) for more

Download details:

IP Address: 129.173.72.87

This content was downloaded on 26/10/2013 at 15:03

Please note that [terms and conditions apply](#).

Swarm dynamics and equilibria for a nonlocal aggregation model

R C Fetecau¹, Y Huang¹ and T Kolokolnikov²

¹ Department of Mathematics, Simon Fraser University, 8888 University Dr., Burnaby, BC V5A 1S6, Canada

² Department of Mathematics and Statistics, Chase Building, Dalhousie University Halifax, NS B3H 3J5, Canada

Received 1 March 2011, in final form 20 July 2011

Published 12 August 2011

Online at stacks.iop.org/Non/24/2681

Recommended by B Eckhardt

Abstract

We consider the aggregation equation $\rho_t - \nabla \cdot (\rho \nabla K * \rho) = 0$ in \mathbb{R}^n , where the interaction potential K models short-range repulsion and long-range attraction. We study a family of interaction potentials for which the equilibria are of finite density and compact support. We show global well-posedness of solutions and investigate analytically and numerically the equilibria and their global stability. In particular, we consider a potential for which the corresponding equilibrium solutions are of uniform density inside a ball of \mathbb{R}^n and zero outside. For such a potential, various explicit calculations can be carried out in detail. In one dimension we fully solve the temporal dynamics, and in two or higher dimensions we show the global stability of this steady state within the class of radially symmetric solutions. Finally, we solve the following restricted inverse problem: given a radially symmetric density $\bar{\rho}$ that is zero outside some ball of radius R and is polynomial inside the ball, construct an interaction potential K for which $\bar{\rho}$ is the steady-state solution of the corresponding aggregation equation. Throughout the paper, numerical simulations are used to motivate and validate the analytical results.

Mathematics Subject Classification: 92D25, 35L65, 35Q92, 35B35

(Some figures in this article are in colour only in the electronic version)

1. Introduction

This paper concerns the study of the following integro-differential aggregation equation in \mathbb{R}^n :

$$\rho_t + \nabla \cdot (\rho v) = 0 \tag{1a}$$

$$v = -\nabla K * \rho. \tag{1b}$$

Here, ρ represents the density of the aggregation, K is the interaction potential and $*$ denotes convolution. The equation appears in various contexts related to mathematical models for biological aggregations; we refer to [1, 2] and references therein for an extensive background and review of the biology literature on this topic. It also arises in a number of other applications such as material science and granular media [3–6], self-assembly of nanoparticles [3, 4] and molecular dynamics simulations of matter [7]. In this work we are only interested in biological applications, where equations (1a) and (1b) can be used to model aggregations such as insect swarms, fish schools, bacterial colonies, etc [1]. The convolution kernel $-\nabla K$ incorporates the endogenous forces arising from the interindividual (attraction and repulsion) interactions [8].

The study of solutions to aggregation models of type (1a) and (1b) has been a very active area of study over the past decade. A significant component of this study has dealt with the well-posedness of the initial-value problem for (1a) and (1b) [9–13]. Another aspect, which is very important due to the biological relevance of the model, is the long time behaviour of solutions to (1a) and (1b). This issue has been addressed in various works. Most of this study deals with solutions that blow up (either in finite or infinite time) by mass concentration into one or several Dirac distributions. The one-dimensional case was investigated in [10, 14, 15] and blow-up in the multidimensional aggregation equation with radially symmetric kernels was studied in [16, 17]. The common feature of these studies is that attraction is the dominating social interaction and repulsion is either absent or too weak to prevent Dirac mass concentrations.

It is essential for an aggregation model to be able to capture solutions with biologically relevant features. As indicated by Mogilner and Keshet in their seminal work [1] on the class of models discussed here, such desired characteristics include finite densities, sharp boundaries, relatively constant internal population and long lifetimes. There is only a handful of works that investigate solutions to (1a) and (1b) which exhibit these realistic features. Topaz and collaborators [8, 14] derived explicit swarm equilibria that arise in the one-dimensional model with Morse-type potentials. Numerical simulations [8] indicate that these equilibria are globally stable, but analytical results supporting this claim are lacking. Furthermore, the explicit calculations from [8, 14] do not extend to higher dimensions. Other works illustrate asymptotic vortex states in 2D [18] and clumps (aggregations with compact support) in a nonlocal model that includes density-dependent diffusion [2].

The main motivation of this study is to provide a more systematic study of solutions to the aggregation model (1a) and (1b) which have the biologically realistic features discussed above. To this purpose we design interaction potentials K for which equilibrium solutions to the aggregation model (1a) and (1b) have these desired characteristics and we investigate analytically and numerically the well-posedness and long time behaviour of solutions. In the rest of this section we give a brief account of the potentials used in this paper and describe the equilibria that they generate.

The analytical and numerical techniques used in this work are rooted in the individual-based description of the model equations (1a) and (1b). More specifically, the PDE model (1a) and (1b) can be regarded as the continuum limit of the following particle (individual-based) model describing the pairwise interaction of N particles in \mathbb{R}^n [8, 19]:

$$\frac{dX_i}{dt} = -\frac{1}{N} \sum_{\substack{j=1 \dots N \\ j \neq i}} \nabla_i K(X_i - X_j), \quad i = 1 \dots N, \quad (2)$$

where $X_i(t)$ represents the spatial location of the i th individual at time t . In the PDE context, the density $\rho(x, t)$ represents a continuum approximation to the distribution of individuals as $N \rightarrow \infty$.

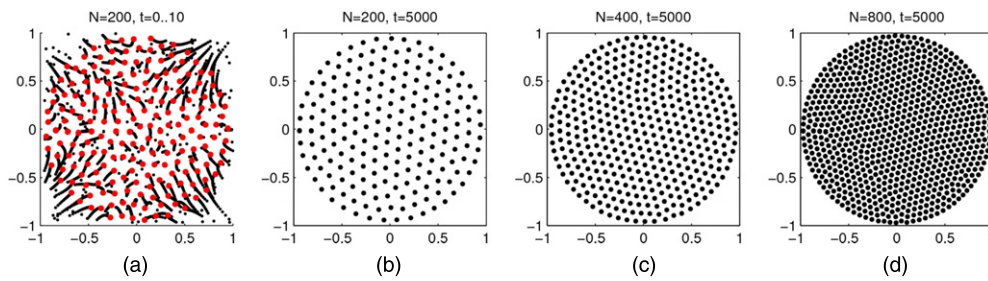


Figure 1. Numerical simulation of (5) in two dimensions and with $F(r) = 1/r - r$. Random initial conditions inside a unit square were used. (a) Evolution of $N = 200$ particles with $t = 0 \dots 10$. (b), (c), (d) Snapshot of the system at $t = 5000$ with N as indicated in the title.

Throughout the paper we assume that social interactions depend only on the relative distance between the individuals and not on their actual locations and hence, consider only radially symmetric potentials,

$$K(x) = K(|x|). \quad (3)$$

Introducing the notation

$$F(r) = -K'(r), \quad (4)$$

we can write the particle system (2) as

$$\frac{dX_i}{dt} = \frac{1}{N} \sum_{\substack{j=1 \dots N \\ j \neq i}} F(|X_i - X_j|) \frac{X_i - X_j}{|X_i - X_j|}, \quad i = 1 \dots N. \quad (5)$$

Note that $F(|X_i - X_j|)$ represents the magnitude of the force that the individual X_j exerts on the individual X_i , along the direction from X_j to X_i . Therefore, the force $F(r)$ must be negative (i.e. attractive) at sufficiently large distances r (otherwise all particles disperse indefinitely), whereas $F(r)$ must be positive (i.e. repulsive) for sufficiently small r to avoid particle collisions. A force that satisfies these conditions is the Morse function [2, 8, 14, 20], where the attraction and repulsion terms are both in the form of decaying exponentials, but of different signs, strengths and length scales. The forces studied in this paper also satisfy the conditions, but are of different forms.

Consider the following repulsive–attractive force in the entire space $\mathbb{R}^n (n \geq 1)$:

$$F(r) = \frac{a}{r^{n-1}} - r, \quad a > 0. \quad (6)$$

The constant a entering the expression of the repulsion component could have been scaled to unity but we leave it in for convenience. Figure 1(a) shows the evolution of the particle model (5) in two dimensions ($n = 2$) with $F(r)$ given by (6) with $a = 1$. The remarkable property of this force function is that solutions approach a steady state for which the density ρ is uniform inside a unit ball, and zero outside. Increasing the number of particles (see figures 1(b)–(d)) does not alter the shape or the radius of the swarm. In a biological setting, such a configuration can be considered optimal, in the sense that no individual within a swarm is favoured over any others, as all are roughly equidistant from their neighbours³.

³ See section 5 for a discussion of how the force (6) can be modified to avoid the biologically unrealistic growth for large or small r .

For convenience of calculations we use in the subsequent sections $a = \frac{1}{n\omega_n}$, where $\omega_n = \frac{\pi^{n/2}}{\Gamma(n/2+1)}$ is the volume of the unit ball in \mathbb{R}^n . The force (6) for this choice of the constant a corresponds to the potential K (see (3) and (4)):

$$K(x) = \phi(x) + \frac{1}{2}|x|^2,$$

where $\phi(x)$ is the free-space Green's function for the negative Laplace operator $-\Delta$:

$$\phi(x) = \begin{cases} -\frac{1}{2}|x|, & n = 1 \\ -\frac{1}{2\pi} \ln |x|, & n = 2 \\ \frac{1}{n(n-2)\omega_n} \frac{1}{|x|^{n-2}}, & n \geq 3. \end{cases} \quad (7)$$

We also consider an extension of this potential, where the repulsion component remains in the form of the Newtonian potential ϕ , but attraction is given by a general power law with exponent $q \geq 2$:

$$K(x) = \phi(x) + \frac{1}{q}|x|^q, \quad q \geq 2. \quad (8)$$

Newtonian (attractive) potentials for model (1a) and (1b) were considered by Du and Zhang [21] in the context of vortex motions in two-dimensional superfluids. Bertozzi *et al* [13] studied the multidimensional aggregation equations (1a) and (1b) with potentials whose singularity at the origin is just 'better' than that of a Newtonian potential (i.e. $K(x) \sim |x|^\alpha$, $\alpha > 2 - n$). A more recent work [22] includes also the critical case $\alpha = 2 - n$. These studies concern, however, concentration and singularity formation in measure-valued solutions. The purpose of our work is very different: we want to consider attractive–repulsive potentials that yield equilibrium states of finite densities and compact support. The attraction component $\frac{1}{q}|x|^q$ of the potential is specifically designed to counter-balance the singular Newtonian repulsion.

Let us summarize the main results of this paper. In section 2 we study the distinguished case $q = 2$ of (8), corresponding to the force (6) with $a = \frac{1}{n\omega_n}$. We first show that in this case the equilibrium density of (1a) and (1b) is uniform inside the ball of radius $R = (n\omega_n)^{-1/n}$ and zero outside the ball. Furthermore, we use the method of characteristics to explicitly solve the full dynamics in one dimension, as well as the dynamics corresponding to radially symmetric initial conditions in any dimension. This shows directly the global stability of the equilibrium in one dimension, as well as the global stability within the class of radially symmetric solutions for any dimension. We also prove global well-posedness of solutions to (1a) and (1b) by borrowing techniques used in the analysis of incompressible fluid flow equations. In section 3 we consider general potentials (8) with $q \geq 2$. The explicit calculations from $q = 2$ do not extend to $q > 2$. We first prove global well-posedness of solutions. By reformulating the equilibrium problem as an eigenvalue problem for an integral operator and applying the Krein–Rutman theorem, we show the existence of a unique radially symmetric equilibrium of compact support. We also derive some more explicit results for the special subcase when q is even. Finally in section 4 we solve the following restricted inverse problem: given a radially symmetric density $\bar{\rho}$ that is zero outside some ball of radius R and is polynomial inside such a ball, construct a corresponding force $F(r)$ for which $\bar{\rho}$ is the equilibrium state. Throughout the paper, numerics are utilized to motivate and validate the analytical results.

2. Constant, compactly supported steady states

We start by making a general observation that the model equations (1a) and (1b) have two important conservation properties. Denote the initial density by ρ_0 :

$$\rho(x, 0) = \rho_0(x), \quad x \in \mathbb{R}^n.$$

The aggregation model (1a) and (1b) satisfies

(i) Conservation of mass:

$$\int \rho(x, t) \, dx = M, \quad \text{for all } t \geq 0, \quad (9)$$

where the constant M denotes the initial mass $M = \int \rho_0(x) \, dx$.

(ii) Conservation of centre of mass:

$$\int x \rho(x, t) \, dx = 0, \quad \text{for all } t \geq 0, \quad (10)$$

where we assumed that without loss of generality, the centre of mass of the initial density is at the origin: $\int x \rho_0(x) \, dx = 0$.

Both properties follow directly from (1a) and (1b). Property (ii) uses the radial symmetry of the potential. The two conservation properties apply to all potentials considered in this paper and will be used frequently.

In this section we study the distinguished case $q = 2$ of (8),

$$K(x) = \phi(|x|) + \frac{1}{2} |x|^2. \quad (11)$$

The equilibria of (1a) and (1b) for this case correspond to constant densities supported on a ball. We use the method of characteristics to solve explicitly the equation in 1D. The explicit calculations extend to radially symmetric solutions in any dimension and yield results regarding global stability of the equilibria. We also investigate the well-posedness of solutions. Only the one and two-dimensional cases are discussed in detail. The higher ($n \geq 3$) dimensional cases can be treated similarly and only the key differences to case $n = 2$ will be highlighted.

We introduce the notation:

$$\begin{aligned} f(x) &= -\nabla K(x) \\ &= F(|x|) \frac{x}{|x|}, \end{aligned}$$

and write the aggregation model as

$$\rho_t + \nabla \cdot (\rho v) = 0 \quad (12a)$$

$$v = f * \rho \quad (12b)$$

$$f(x) = \left(\frac{1}{n\omega_n} \frac{1}{|x|^{n-1}} - |x| \right) \frac{x}{|x|}. \quad (12c)$$

2.1. One dimension ($n = 1$)

We will show that the following constant, compactly supported steady state is a global attractor for solutions of (12a)–(12c) when $n = 1$:

$$\bar{\rho}(x) = \begin{cases} M & \text{if } |x| < \frac{1}{2} \\ 0 & \text{otherwise.} \end{cases} \quad (13)$$

It is easy to check that $\bar{\rho}$ defined above is a steady state. Indeed, calculation of $\bar{v} = f * \bar{\rho}$, with f given by (12c) (for $n = 1$, $\omega_1 = 2$), yields:

$$\bar{v}(x) = 0, \quad \text{for all } |x| < \frac{1}{2}.$$

Note that $\bar{\rho} = 0$ for $|x| > \frac{1}{2}$, which implies $\bar{\rho}\bar{v} = 0$ a.e. in \mathbb{R} . It is then easy to check that $\bar{\rho}$ is indeed a (steady) weak solution of the conservation law (12a)–(12c).

We show that $\bar{\rho}$ is a global attractor by calculating an explicit solution to (12a)–(12c) when $n = 1$. Indeed, compute v , with f given by (12c). We find

$$v(x, t) = \int_{-\infty}^x \rho(y, t) dy - M \left(x + \frac{1}{2} \right), \quad (14)$$

where we used conservation of mass (9) and conservation of centre of mass (10).

Using (14), the one-dimensional model equation (12a)–(12c) can be written as

$$\begin{aligned} \rho_t + v\rho_x &= -v_x\rho \\ &= -\rho(\rho - M). \end{aligned}$$

Define the characteristics $X(\alpha, t)$ that originate from α at $t = 0$:

$$\frac{d}{dt}X(\alpha, t) = v(X(\alpha, t), t), \quad X(\alpha, 0) = \alpha. \quad (15)$$

Along characteristics, $\rho(X(\alpha, t), t)$ satisfies

$$\frac{D}{Dt}\rho = -\rho(\rho - M).$$

This ODE has a solution that asymptotically approaches the value M as $t \rightarrow \infty$. In fact, ρ along characteristics can be computed explicitly:

$$\rho(X(\alpha, t), t) = \frac{M}{1 + \left(\frac{M}{\rho_0(\alpha)} - 1 \right) e^{-Mt}}.$$

We solve now for the characteristic paths. Denote

$$w(x, t) = \int_{-\infty}^x \rho(y, t) dy.$$

Use (14) and (15) to obtain

$$\frac{d}{dt}X(\alpha, t) = w(X(\alpha, t), t) - M \left(X(\alpha, t) + \frac{1}{2} \right).$$

Integrate the one-dimensional version of the model equation (12a) from $-\infty$ to x to find that w satisfies

$$w_t + \left(w - M \left(x + \frac{1}{2} \right) \right) w_x = 0.$$

Infer from the last two equations that w is constant along the characteristic paths:

$$w(X(\alpha, t), t) = w(\alpha, 0).$$

The characteristic equation can now be written as

$$\frac{d}{dt}X(\alpha, t) = w(\alpha, 0) - M \left(X(\alpha, t) + \frac{1}{2} \right).$$

This ODE (with initial condition $X(\alpha, 0) = \alpha$) can be solved exactly. The solution is given by

$$X(\alpha, t) = e^{-Mt}\alpha + \frac{1}{M} (1 - e^{-Mt}) \left(w(\alpha, 0) - \frac{M}{2} \right).$$

As $t \rightarrow \infty$, $X(\alpha, t) \rightarrow \frac{1}{M}w(\alpha, 0) - \frac{1}{2}$. Therefore, the real line $(-\infty, \infty)$ is mapped into $(\frac{1}{M}w(-\infty, 0) - \frac{1}{2}, \frac{1}{M}w(\infty, 0) - \frac{1}{2})$. From the definition of w , $w(-\infty, 0) = 0$ and $w(\infty, 0) = M$, hence the characteristics asymptotically approach the interval $(-\frac{1}{2}, \frac{1}{2})$. As ρ along any characteristic path approaches the value M as $t \rightarrow \infty$, we conclude that $\bar{\rho}$ given by (13) is a global attractor for the 1D model equation.

2.2. Two dimensions ($n = 2$)

In this subsection we investigate the solutions to the model equation (12a)–(12c), for $n = 2$. We derive *a priori* estimates and establish local and global existence and uniqueness of solutions. Finally, assuming radial symmetry, we prove that solutions approach asymptotically a steady state given by a constant density supported on a disc:

$$\bar{\rho}(x) = \begin{cases} 2M & \text{if } |x| < \frac{1}{\sqrt{2\pi}} \\ 0 & \text{otherwise.} \end{cases} \quad (16)$$

To show that $\bar{\rho}$ is a steady state of (12a)–(12c), note first that with K as given by (11),

$$\Delta_x \left(\int_{\mathbb{R}^2} K(x-y)\bar{\rho}(y) dy \right) = 0 \quad \text{in } |x| < \frac{1}{\sqrt{2\pi}}.$$

Using radial symmetry we conclude that

$$\int_{\mathbb{R}^2} K(x-y)\bar{\rho}(y) dy = \text{const.} \quad \text{in } |x| < \frac{1}{\sqrt{2\pi}}.$$

Hence, by differentiation, $\bar{v} = -\nabla K * \bar{\rho}$ vanishes inside the disc:

$$\bar{v}(x) = 0 \quad \text{in } |x| < \frac{1}{\sqrt{2\pi}}.$$

Since $\bar{\rho} = 0$ for $|x| > \frac{1}{\sqrt{2\pi}}$, $\bar{\rho}\bar{v} = 0$ a.e. in \mathbb{R}^2 . Hence, $\bar{\rho}$ is a (steady) weak solution of (12a)–(12c).

We prove at the end of this subsection that $\bar{\rho}$ is a global attractor for radially symmetric solutions. Numerical results (see for example figure 1) indicate, however, that $\bar{\rho}$ is also a global attractor for solutions that are not radially symmetric.

2.3. Properties of solutions to (12a)–(12c)

Bounds on the density. Calculate v from (12b) and (12c) ($n = 2$, $\omega_2 = \pi$) using conservation of mass (9) and conservation of centre of mass (10):

$$\begin{aligned} & \int_{\mathbb{R}^2} \left(\frac{1}{2\pi} \frac{1}{|x-y|} - |x-y| \right) \frac{x-y}{|x-y|} \rho(y) dy \\ &= \frac{1}{2\pi} \int_{\mathbb{R}^2} \frac{x-y}{|x-y|^2} \rho(y) dy - x \underbrace{\int_{\mathbb{R}^2} \rho(y) dy}_{=M} + \underbrace{\int_{\mathbb{R}^2} y\rho(y) dy}_{=0} \end{aligned}$$

Hence,

$$v(x) = \int_{\mathbb{R}^2} k(x-y)\rho(y) dy - Mx, \quad (17)$$

where

$$k(x) = \frac{1}{2\pi} \left(\frac{x_1}{|x|^2}, \frac{x_2}{|x|^2} \right). \quad (18)$$

The convolution kernel k is singular, homogeneous of degree -1 . A kernel with similar properties appears in the Biot–Savart law for incompressible fluids, which provides a nonlocal expression for velocity in terms of vorticity. The analogy with the Biot–Savart law will be heavily used below to show existence and uniqueness of solutions to our aggregation model. Analogies with incompressible fluid flow have also been made in the context of Keller–Segel models, where the chemical concentration can be expressed as a convolution of the Newtonian potential with the organism density [23].

Using

$$k(x) = \nabla_x \left(\frac{1}{2\pi} \log |x| \right),$$

one can derive from (17):

$$\nabla \cdot v = \rho - 2M. \quad (19)$$

Expand $\nabla \cdot (\rho v) = v \cdot \nabla \rho + \rho \nabla \cdot v$, and write the aggregation equation (12a) as

$$\rho_t + v \cdot \nabla \rho = -\rho(\rho - 2M).$$

Along characteristics,

$$\frac{d}{dt} X(\alpha, t) = v(X(\alpha, t), t), \quad X(\alpha, 0) = \alpha, \quad (20)$$

$\rho(X(\alpha, t), t)$ satisfies

$$\frac{D}{Dt} \rho = -\rho(\rho - 2M). \quad (21)$$

This ODE has a solution that approaches the value $2M$ as $t \rightarrow \infty$, along *all* characteristic paths that transport non-zero densities. In fact, a solution of (21) can be computed explicitly. Along characteristics, ρ is given by

$$\rho(X(\alpha, t), t) = \frac{2M}{1 + \left(\frac{2M}{\rho_0(\alpha)} - 1 \right) e^{-2Mt}}, \quad (22)$$

where ρ_0 is the initial density.

There are two important conclusions that can be inferred from (22).

- (i) (*Bounds on density*) Equation (22) provides an upper bound on the density ρ , for as long as the particle map exists:

$$\|\rho(\cdot, t)\|_{L^\infty} \leq \frac{2M}{1 + \left(\frac{2M}{\|\rho_0\|_{L^\infty}} - 1 \right) e^{-2Mt}}.$$

We can also derive a uniform bound in time:

$$\|\rho(\cdot, t)\|_{L^\infty} \leq \max \{ \|\rho_0\|_{L^\infty}, 2M \}, \quad \text{for all } t. \quad (23)$$

- (ii) (*Bounds on Jacobian*) The continuity equation (12a) expresses the fact that

$$\rho(X(\alpha, t), t) J(\alpha, t) = \rho_0(\alpha), \quad (24)$$

where

$$J(\alpha, t) = \det \nabla_\alpha X$$

is the Jacobian of the particle map $\alpha \rightarrow X(\alpha, t)$. Using (22), we compute

$$J(\alpha, t) = \frac{\rho_0(\alpha)}{2M} + \left(1 - \frac{\rho_0(\alpha)}{2M} \right) e^{-2Mt}. \quad (25)$$

Note that

$$J(\alpha, t) > 0 \quad \text{for all } t,$$

guaranteeing that the particle map $\alpha \rightarrow X(\alpha, t)$ is invertible for as long as it exists.

Bounds on the support. We show that solutions of (12a)–(12c) are compactly supported provided the initial density ρ_0 is. The density is transported along characteristics according to (24), so it is enough to show that the trajectories $X(\alpha, t)$ that carry non-zero densities remain within some compact set.

Calculate using (17) and (18):

$$x \cdot v(x) = x \cdot \frac{1}{2\pi} \int \frac{x-y}{|x-y|^2} \rho(y) dy - M|x|^2. \quad (26)$$

We isolate the singularity at the origin of the convolution kernel and estimate

$$\begin{aligned} x \cdot \int \frac{x-y}{|x-y|^2} \rho(y, t) dy &= \int_{|y-x|<1} \frac{x \cdot (x-y)}{|x-y|^2} \rho(y, t) dy + \int_{|y-x|>1} \frac{x \cdot (x-y)}{|x-y|^2} \rho(y, t) dy \\ &\leq \|\rho(\cdot, t)\|_{L^\infty} |x| \int_{|y-x|<1} \frac{1}{|x-y|} dy + |x| \int_{|y-x|>1} \rho(y, t) dy \\ &\leq (2\pi \|\rho(\cdot, t)\|_{L^\infty} + \|\rho(\cdot, t)\|_{L^1}) |x|. \end{aligned} \quad (27)$$

Suppose that the solution ρ has remained compactly supported in a disc of radius R up to time t (equivalently, the particle trajectories $X(\alpha, s)$, $s \leq t$, that carried non-zero densities have been contained in the disc of radius R). Assume t large enough such that $\|\rho(\cdot, t)\|_{L^\infty} \leq 4M$ (see comment (i) above regarding bounds on density). Hence, the previous inequality (also use $\|\rho(\cdot, t)\|_{L^1} = M$) yields

$$x \cdot \int \frac{x-y}{|x-y|^2} \rho(y, t) dy \leq (8\pi + 1)M|x|.$$

Use (26) for $x = X(\alpha, t)$ and infer

$$\frac{d}{dt} |X(\alpha, t)| \leq \left(4 + \frac{1}{2\pi}\right) M - M|X(\alpha, t)|.$$

Hence, provided

$$4 + \frac{1}{2\pi} < R,$$

the trajectories that carry non-zero densities will remain inside the disc of radius R .

Existence and uniqueness of solutions. Make the change of variable $y = X(\beta, t)$ and use (24) to write the characteristic equation (20) as

$$\frac{d}{dt} X(\alpha, t) = \frac{1}{2\pi} \int_{\mathbb{R}^2} \frac{X(\alpha, t) - X(\beta, t)}{|X(\alpha, t) - X(\beta, t)|^2} \rho_0(\beta) d\beta - MX(\alpha, t) \quad (28a)$$

$$X(\alpha, 0) = \alpha. \quad (28b)$$

We regard (28a) and (28b) as an ODE on a certain Banach space and show the local existence and uniqueness by invoking the standard Picard theorem. The choice of the Banach space and the setup of the ODE framework is the same as that presented in chapter 4 of [24] in the context of incompressible flow. In [24], the particle-trajectory method is used to show existence and uniqueness of incompressible Euler equations in 2 and 3 dimensions. The Biot–Savart law for incompressible fluids expresses the velocity v as a space convolution of a kernel K with vorticity ω . The convolution kernel K is singular, homogeneous of degree $1-n$ (n is the number of dimensions), i.e. $K(\lambda x) = \lambda^{1-n} K(x)$, for all $\lambda > 0$, $x \neq 0$. This property of the kernel plays a central role in the analysis and the ODE setup from [24]. Another important aspect of the analysis presented in [24] is how the global existence of solutions is linked to the accumulation of vorticity $\int_0^t \|\omega(\cdot, s)\|_{L^\infty} ds$ (Beale–Kato–Majda condition [25]). In particular,

global existence can be inferred in 2 dimensions, since vorticity is preserved along particle paths.

We describe below how the incompressible fluid framework extends to the particle system (28a) and (28b). In (12b) the velocity is expressed as a convolution, where the role of vorticity is played now by the density ρ . The first main observation is that the convolution kernel in (28a) and (28b) is homogeneous of degree -1 ($1 - n$ in n dimensions), as is the kernel in the Biot–Savart law. The second main observation relates to the Beale–Kato–Majda condition. Due to previous considerations, the density ρ is uniformly bounded in time (the result holds in any dimension as well), guaranteeing global existence of solutions. To avoid an unnecessarily long presentation of the existence and uniqueness results, we will make reference to [24] for all technical lemmas and theorems. There are a few key aspects that are different from incompressible fluids (the fact that the flow of (28a) and (28b) is not divergence-free for instance) which will be highlighted appropriately.

Write (28a) and (28b) as

$$\frac{d}{dt} X(\alpha, t) = \mathcal{F}(X(\alpha, t)) \quad (29a)$$

$$X(\alpha, 0) = \alpha, \quad (29b)$$

where the map $\mathcal{F}(X)$ is defined by

$$\mathcal{F}(X(\alpha, t)) = \frac{1}{2\pi} \int_{\mathbb{R}^2} \frac{X(\alpha, t) - X(\beta, t)}{|X(\alpha, t) - X(\beta, t)|^2} \rho_0(\beta) d\beta - MX(\alpha, t). \quad (30)$$

Following [24], we consider the Banach space

$$\mathcal{B} = \{X : \mathbb{R}^2 \rightarrow \mathbb{R}^2 \text{ such that } \|X\|_{1,\gamma} < \infty\},$$

where $\|\cdot\|_{1,\gamma}$ is the norm defined by

$$\|X\|_{1,\gamma} = |X(0)| + \|\nabla_\alpha X\|_{L^\infty} + |\nabla_\alpha X|_\gamma. \quad (31)$$

Here, $|\cdot|_\gamma$ is the Hölder seminorm

$$|\nabla_\alpha X|_\gamma = \sup_{\alpha \neq \alpha'} \frac{|\nabla_\alpha X(\alpha) - \nabla_\alpha X(\alpha')|}{|\alpha - \alpha'|^\gamma}.$$

Consider an open subset \mathcal{O}_L of \mathcal{B} , defined by

$$\mathcal{O}_L = \left\{ X \in \mathcal{B} \mid \inf_\alpha \det \nabla_\alpha X(\alpha) > 1/L \text{ and } \|X\|_{1,\gamma} < L \right\}.$$

The local existence and uniqueness is stated by the following theorem.

Theorem 2.1 (Local existence and uniqueness). *Consider a compactly supported initial density $\rho_0 \in L^\infty(\mathbb{R}^2)$, with $|\rho_0|_\gamma < \infty$, for some $\gamma \in (0, 1)$. Then for any $L > 0$, there exists $T(L) > 0$ and a unique solution $X \in C^1((-T(L), T(L)); \mathcal{O}_L)$ to (29a)–(30).*

Proof. The proof follows from Picard’s theorem, provided \mathcal{F} is shown to be bounded and locally Lipschitz continuous on \mathcal{O}_L . The expression for \mathcal{F} from (30) contains a linear term (which presents no difficulties) and a convolution of a singular kernel of degree -1 with the initial density ρ_0 . To show that \mathcal{F} is bounded and Lipschitz continuous one can follow the same steps as in the proof of proposition 4.2, chapter 4.1 in [24]. The key ingredients used in that proof are the degrees of homogeneity of the kernel and its gradient; the specific form of the kernel is not used in fact. The gradient of the kernel is homogeneous of degree -2 and defines a singular integral operator (SIO). It is specifically the limited properties of these singular kernels that bring the need for the Hölder γ -seminorm used in (31). See the appendix for an outline of the proof. \square

We now use a continuation result of solutions to autonomous ODEs on Banach spaces (theorem 4.4 in [24]) to upgrade the result to global existence. Inspecting the set \mathcal{O}_L we infer that we cease to have a solution at a finite time T_* provided either $\inf_{\alpha} \det \nabla_{\alpha} X(\alpha)$ becomes 0 or $\|X\|_{1,\gamma}$ becomes unbounded as $t \rightarrow T_*$.

The first scenario is ruled out by the following proposition.

Proposition 2.2. *At any fixed time $t < \infty$, solutions of (29a)–(30) satisfy*

$$\inf_{\alpha} \det \nabla_{\alpha} X(\alpha, t) \geq e^{-2Mt}.$$

Proof. The proof is a direct consequence of the explicit calculation of the Jacobian J . From (25) we derive, at any time t :

$$J(\alpha, t) \geq e^{-2Mt}, \quad \text{for all } \alpha.$$

The conclusion of the proposition then follows. \square

The second scenario for the break-up of the solution (finite-time blow-up of $\|X\|_{1,\gamma}$) will be treated as in chapter 4.2 of [24].

Proposition 2.3. *Provided $\int_0^t \|\nabla v(\cdot, s)\|_{L^\infty}$ has an a priori bound, $\|\nabla_{\alpha} X(\cdot, t)\|_{L^\infty}$ and $|\nabla_{\alpha} X(\cdot, t)|_{\gamma}$ are a priori bounded.*

Proof. See the appendix. \square

For incompressible fluids, global existence of solutions is linked to the Beale–Kato–Majda condition [25]. More specifically, a sufficient condition for global existence is an a priori control on the time-integral of the supremum norm of vorticity. In the context of our aggregation model (29a)–(30), this condition will be replaced by an a priori bound on $\int_0^t \|\rho(\cdot, s)\|_{L^\infty} ds$.

Lemma 2.4. *A sufficient condition for $\int_0^t \|\nabla v(\cdot, s)\|_{L^\infty} ds$ to be a priori bounded is an a priori bound on $\int_0^t \|\rho(\cdot, s)\|_{L^\infty} ds$. More specifically,*

$$\int_0^t \|\nabla v(\cdot, s)\|_{L^\infty} ds \leq e^{C(\rho_0) \int_0^t \|\rho(\cdot, s)\|_{L^\infty} ds},$$

where $C(\rho_0)$ is a constant that depends on the initial density only.

Proof. In the context of incompressible fluids, the corresponding statement, i.e. $\int_0^t \|\omega(\cdot, s)\|_{L^\infty} ds$ controls $\int_0^t \|\nabla v(\cdot, s)\|_{L^\infty} ds$, is the key ingredient for linking the global existence with the Beale–Kato–Majda condition (see [25] or theorem 4.3 in [24]). Its proof can be trivially adapted to our problem, with density ρ now replacing vorticity ω . We omit the details. \square

Finally, we have all the ingredients to prove global existence of solutions. The result is given by the following theorem.

Theorem 2.5 (Global existence). *Consider an initial density ρ_0 as in theorem 2.1. Then, for every T , there exists $L > 0$ and a unique solution $X \in C^1([0, T]; \mathcal{O}_L)$ to (29a)–(30) (the solution exists globally in time).*

Proof. The solution X is in the set \mathcal{O}_L provided

$$\inf_{\alpha} \det \nabla_{\alpha} X(\alpha) > 1/L \quad \text{and} \quad \|X\|_{1,\gamma} < L. \tag{32}$$

Using proposition 2.2, the first condition is satisfied provided we choose $L > e^{2MT}$. We now investigate the second condition in (32). Start by inspecting the first term in (31), $|X(0, t)|$. Integrate (20) to obtain

$$X(0, t) = \int_0^t v(X(0, s), s) \, ds. \tag{33}$$

Recall that the expression for velocity $v(x)$ in (17) has two components: the convolution of the singular kernel k of degree -1 with ρ , and $-Mx$. To estimate the first component of v , we use lemma 4.5 in chapter 4 [24] and find

$$\|k * \rho\|_{L^{\infty}} \leq c\sqrt{R}\|\rho\|_{L^{\infty}},$$

where c is a constant and R is the radius of the ball that contains the support of ρ —the existence of such a ball was shown above, in the paragraph that discusses the uniform, compact support of the density. Hence, from (33), we find

$$|X(0, t)| \leq c\sqrt{R} \int_0^t \|\rho(\cdot, s)\|_{L^{\infty}} \, ds + M \int_0^t |X(0, s)| \, ds.$$

Gronwall’s lemma yields

$$|X(0, t)| \leq c\sqrt{R} \int_0^t \|\rho(\cdot, s)\|_{L^{\infty}} e^{M(t-s)} \, ds. \tag{34}$$

The control of $\|X\|_{1,\gamma}$ now follows from (34), (105), (108) and lemma 2.4. More precisely, by redefining the constants appropriately, one can derive

$$\|X(\cdot, t)\|_{1,\gamma} \leq C e^{C_1 t} e^{C_2 e^{C_3 \int_0^t \|\rho(\cdot, s)\|_{L^{\infty}} \, ds}}. \tag{35}$$

Using the uniform bound (23) on $\|\rho(\cdot, s)\|_{L^{\infty}}$ we observe that we can choose the constant L large enough such that $\|X(\cdot, t)\|_{1,\gamma} < L$, for all $t \in [0, T]$. □

Asymptotic behaviour of solutions. We study the asymptotic behaviour of radially symmetric solutions and prove the following result:

Theorem 2.6. *Consider a radially symmetric initial density ρ_0 satisfying the hypotheses of theorem 2.5. Then, the global solution ρ of the 2D aggregation model (12a)–(12c) remains radially symmetric for all times and approaches asymptotically, as $t \rightarrow \infty$, the steady state (16).*

Proof. It is easy to show that, due to the radial symmetry of the interaction kernel, the density remains radially symmetric for all times. For radially symmetric solutions, the velocity at a point x has magnitude that depends on $|x|$ and direction $\frac{x}{|x|}$. Consequently, the trajectory that emanates from a particle α is a straight line in the direction α :

$$X(\alpha, t) = \lambda(|\alpha|, t)\alpha, \tag{36}$$

where λ is a function that has to be determined.

Using (36), we compute the Jacobian $J = \det \nabla_{\alpha} X$:

$$J(\alpha, t) = \lambda(|\alpha|, t)(\lambda(|\alpha|, t) + \lambda_r(|\alpha|, t)|\alpha|),$$

where the subindex r indicates the derivative with respect to the first (radial) coordinate. The initial density is radially symmetric, $\rho_0(\alpha) = \rho_0(r)$, where $r = |\alpha|$. Using the exact formula (25) for J we arrive at an ODE for λ :

$$\lambda^2 + \lambda \lambda_{,r} r = \frac{\rho_0(r)}{2M} + \left(1 - \frac{\rho_0(r)}{2M}\right) e^{-2Mt}.$$

Multiply by the integrating factor $2r$ to obtain:

$$\frac{d}{dr} (r^2 \lambda^2) = 2r \left(\frac{\rho_0(r)}{2M} + \left(1 - \frac{\rho_0(r)}{2M}\right) e^{-2Mt} \right).$$

Integrate from 0 to r to find

$$r^2 \lambda^2 = \frac{1}{M} \int_0^r s \rho_0(s) ds + 2e^{-2Mt} \int_0^r s \left(1 - \frac{\rho_0(s)}{2M}\right) ds. \quad (37)$$

Denote

$$R_\alpha = \lim_{t \rightarrow \infty} |X(\alpha, t)|. \quad (38)$$

Pass $t \rightarrow \infty$ in (37) and use (36) to obtain

$$R_\alpha^2 = \frac{1}{M} \int_0^{|\alpha|} s \rho_0(s) ds.$$

Note, however, that the mass M can be written in polar coordinates as

$$M = 2\pi \int_0^\infty s \rho_0(s) ds.$$

Therefore, $R_\alpha \leq \frac{1}{\sqrt{2\pi}}$ for all α and clearly, for α large, outside the support of ρ_0 , $R_\alpha = \frac{1}{\sqrt{2\pi}}$. This shows that the disc of radius $1/\sqrt{2\pi}$ is a global attractor for trajectories. From (22), $\rho \rightarrow 2M$ as $t \rightarrow \infty$, along any particle path. Combining the two results we infer that radial solutions to the 2D aggregation model (12a)–(12c) approach asymptotically the compactly supported steady state (16). \square

2.4. Higher dimensions ($n \geq 3$)

All calculations and results from the previous subsection extend to general n dimensions. We mention briefly the key differences. The velocity v reads

$$v(x) = \int_{\mathbb{R}^n} k(x-y) \rho(y) dy - Mx, \quad (39)$$

where

$$k(x) = \frac{1}{n\omega_n} \frac{x}{|x|^n}. \quad (40)$$

The convolution kernel k is singular, homogeneous of degree $1-n$. Existence and uniqueness results follow as in 2D, via the analogy with incompressible fluid equations. Using

$$\nabla \cdot v = \rho - nM$$

we can write the model equation (12a) along characteristics as

$$\frac{D}{Dt} \rho = -\rho(\rho - nM).$$

This ODE has a solution that approaches the value nM as $t \rightarrow \infty$, along *all* characteristic paths that carry non-zero density values. A solution can be computed exactly:

$$\rho(X(\alpha, t), t) = \frac{nM}{1 + \left(\frac{nM}{\rho_0(\alpha)} - 1\right) e^{-nMt}},$$

where ρ_0 is the initial density. The density is uniformly bounded in time:

$$\|\rho(\cdot, t)\|_{L^\infty} \leq \max \{\|\rho_0\|_{L^\infty}, nM\}, \quad \text{for all } t.$$

The Jacobian of the particle map $\alpha \rightarrow X(\alpha, t)$ can also be computed:

$$J(\alpha, t) = \frac{\rho_0(\alpha)}{nM} + \left(1 - \frac{\rho_0(\alpha)}{nM}\right) e^{-nMt}. \tag{41}$$

For radially symmetric solutions, using (36), one finds

$$J(\alpha, t) = \lambda^{n-1}(|\alpha|, t)(\lambda(|\alpha|, t) + \lambda_r(|\alpha|, t)|\alpha|).$$

Use the exact formula for J to arrive at an ODE for λ :

$$\lambda^n + \lambda^{n-1}\lambda_r r = \frac{\rho_0(r)}{nM} + \left(1 - \frac{\rho_0(r)}{nM}\right) e^{-nMt}.$$

Solve by integrating factor nr^{n-1} to obtain:

$$r^n \lambda^n = \frac{1}{M} \int_0^r s^{n-1} \rho_0(s) ds + ne^{-nMt} \int_0^r s^{n-1} \left(1 - \frac{\rho_0(s)}{nM}\right) ds \tag{42}$$

Hence, we compute the asymptotic radius R_α (see (38)):

$$R_\alpha^n = \frac{1}{M} \int_0^{|\alpha|} s^{n-1} \rho_0(s) ds.$$

Since $M = n\omega_n \int_0^\infty s^{n-1} \rho_0(s) ds$, we find that $R_\alpha \leq \frac{1}{(n\omega_n)^{\frac{1}{n}}}$ for all α . Particles at infinity are mapped on the n -sphere of radius $R_\alpha = \frac{1}{(n\omega_n)^{\frac{1}{n}}}$.

We conclude that radial solutions to the n -dimensional aggregation model (12a)–(12c) approach asymptotically the compactly supported steady state given by

$$\bar{\rho}(x) = \begin{cases} nM & \text{if } |x| < \frac{1}{(n\omega_n)^{\frac{1}{n}}} \\ 0 & \text{otherwise.} \end{cases} \tag{43}$$

3. Non-constant, compactly supported steady states

In this section we study the aggregation model (1a), (1b) and (8), with ϕ given by (7), for exponents $q > 2$. Note that most of the explicit calculations from section 2 do not apply for general q 's. We are able to show that, for exponents $q > 2$, the amplitude and support of solutions to the aggregation model remain uniformly bounded in time. As a consequence, existence and uniqueness results from the previous section extend to $q > 2$. We also investigate the radially symmetric steady states. For every $q > 2$, a unique radially symmetric, compactly supported steady state can be shown to exist analytically. When q is even we show that these equilibria are polynomials of even powers of the radial coordinate r . Finally, we describe a procedure to calculate numerically the radially symmetric steady states for general $q > 2$ and provide numerical evidence that these steady states are global attractors for the dynamics of (1a) and (1b).

3.1. Properties of solutions

For convenience, we restate the aggregation model for general exponent q :

$$\rho_t + \nabla \cdot (\rho v) = 0 \quad (44a)$$

$$v = f * \rho \quad (44b)$$

$$f(x) = \left(\frac{1}{n\omega_n} \frac{1}{|x|^{n-1}} - |x|^{q-1} \right) \frac{x}{|x|}. \quad (44c)$$

Bounds on the density and its support. Calculate from (44b) and (44c):

$$\nabla \cdot v = \rho - (n + q - 2) \int_{\mathbb{R}^n} |x - y|^{q-2} \rho(y) \, dy. \quad (45)$$

Hence, along characteristics, the density $\rho(X(\alpha, t), t)$ satisfies

$$\frac{D}{Dt} \rho = -\rho \left(\rho - (n + q - 2) \int_{\mathbb{R}^n} |X(\alpha, t) - X(\beta, t)|^{q-2} \rho_0(\beta) \, d\beta \right). \quad (46)$$

Note that this is no longer a local equation, as for $q = 2$ (see (21) for instance). The ODE (46) now depends explicitly on the particle trajectories and in particular, on the support of the density. Nevertheless, we can still show that, provided the density and its support are bounded initially, they remain uniformly bounded for all times.

At time t , define the maximum density $\rho_{\max}(t)$ and the maximum radius of support $R(t)$ as

$$\rho_{\max}(t) = \max_{\alpha} \rho(\alpha, t), \quad R(t) = \max_{\alpha: \rho_0(\alpha) \neq 0} |X(\alpha, t)|. \quad (47)$$

From (46), an inequality for ρ_{\max} can be easily obtained:

$$\frac{d\rho_{\max}}{dt} \leq ((n + q - 2)(2R(t))^{q-2} M - \rho_{\max}) \rho_{\max}. \quad (48)$$

Regarding estimates on the support radius $R(t)$ we proceed similarly to the case $q = 2$ and calculate using (44b) and (44c):

$$x \cdot v(x, t) = \int_{\mathbb{R}^n} \frac{x \cdot (x - y)}{n\omega_n |x - y|^n} \rho(y, t) \, dy - \int_{\mathbb{R}^n} x \cdot (x - y) |x - y|^{q-2} \rho(y, t) \, dy. \quad (49)$$

The first term in the right-hand side of (49) can be bounded similarly to (27). For any fixed $r_* > 0$, we have

$$\begin{aligned} \int_{\mathbb{R}^n} \frac{x \cdot (x - y)}{n\omega_n |x - y|^n} \rho(y, t) \, dy &= \int_{|x-y| < r_*} \frac{x \cdot (x - y)}{n\omega_n |x - y|^n} \rho(y, t) \, dy \\ &\quad + \int_{|x-y| > r_*} \frac{x \cdot (x - y)}{n\omega_n |x - y|^n} \rho(y, t) \, dy \\ &\leq \frac{\rho_{\max}(t)|x|}{n\omega_n} \int_{|x-y| < r_*} \frac{1}{|x - y|^{n-1}} \, dy \\ &\quad + \frac{|x|}{n\omega_n r_*^{n-1}} \int_{|x-y| > r_*} \rho(y, t) \, dy \\ &\leq \left(\rho_{\max}(t)r_* + \frac{M}{n\omega_n r_*^{n-1}} \right) |x| \\ &= \frac{n+1}{n} \left(\frac{M}{\omega_n} \right)^{1/n} \rho_{\max}^{1-\frac{1}{n}} |x|, \end{aligned} \quad (50)$$

where we chose $r_* = (M/(\omega_n \rho_{\max}))^{1/n}$ in the last step.

The second term in the right-hand side of (49) can be bounded by restricting to those trajectories $X(\alpha, t)$ on the boundary of the support, i.e. $|X(\alpha, t)| = R(t) \geq |X(\beta, t)|$ for any β such that $\rho_0(\beta) > 0$. We need the following lemma.

Lemma 3.1. *There exists a constant c , depending only on the dimension of the space such that for any nonnegative, compactly supported measure μ on \mathbb{R}^n with total mass M and centre of mass at the origin, we have*

$$\int_{\mathbb{R}^n} x \cdot (x - y)|x - y|^{q-2} d\mu(y) \geq c|x|^q M, \quad (51)$$

for any x with $|x| \geq R$, where R is the radius of the support of μ .

Proof. Suppose there is no constant c with such properties. Then there exists a sequence of points $\{x_m\}$ and nonnegative measures $\{\mu_m\}$ of total mass M and centre of mass at the origin such that

$$\int_{\mathbb{R}^n} x_m \cdot (x_m - y)|x_m - y|^{q-2} d\mu_m(y) < \frac{1}{m}|x_m|^q M, \quad (52)$$

where $|x_m| \geq R_m$ and R_m is the radius of the support. Since above inequality (52) is invariant under the scaling on the space $x_m \rightarrow x_m/|x_m|$, $y \rightarrow y/|x_m|$ and on the measure $\mu_m(y) \rightarrow \mu_m(y/|x_m|)/|x_m|^n$, we can assume that $|x_m| = 1$ and $R_m \leq 1$. By the compactness of the sequence $\{x_m\}$ and the weak compactness of the measures $\{\mu_m\}$, there exist subsequences $\{x_{m_k}\}$ and $\{\mu_{m_k}\}$ such that x_{m_k} converges to x_0 with $|x_0| = 1$ and μ_{m_k} converges to μ_0 . In particular, μ_0 has the centre of mass at the origin. Passing the limit in (52) when m_k goes to infinity,

$$\begin{aligned} \int_{\mathbb{R}^n} x_0 \cdot (x_0 - y)|x_0 - y|^{q-2} d\mu_0(y) &= \lim_{m_k \rightarrow \infty} \int_{\mathbb{R}^n} x_0 \cdot (x_0 - y)|x_0 - y|^{q-2} d\mu_{m_k}(y) \\ &\leq \lim_{m_k \rightarrow \infty} \frac{1}{m_k}|x_0|^q M = 0. \end{aligned}$$

This implies that μ_0 is the delta measure concentrated at x_0 , and therefore has the centre of mass at x_0 . This contradicts the fact that μ_0 has centre of mass at the origin. \square

Remark. The constant c can be calculated explicitly (although not always optimal) in the special cases when q is positive and even. For $q = 2$,

$$\int_{\mathbb{R}^n} x \cdot (x - y)\rho(y) dy = |x|^2 M,$$

with $c = 1$. For $q = 4$,

$$\begin{aligned} \int_{\mathbb{R}^n} x \cdot (x - y)|x - y|^2 \rho(y) dy \\ = \int_{\mathbb{R}^n} (|x|^4 + |x|^2|y|^2 + 2(x \cdot y)^2 - (x \cdot y)|y|^2)\rho(y) dy \geq |x|^4 M, \end{aligned}$$

with $c = 1$ (although not necessary optimal).

Using (50) and (51) in (49) for $x = X(\alpha, t)$ on the boundary of the support, we find the differential inequality

$$\frac{dR}{dt} \leq \frac{n+1}{n} \left(\frac{M}{\omega_n}\right)^{1/n} \rho^{1-\frac{1}{n}} - cMR^{q-1}. \quad (53)$$

Now inspect (48) and (53). If initially the maximum density $\rho_{\max}(0)$ and the radius of the support $R(0)$ are bounded, then there exist $\tilde{\rho} \geq \rho_{\max}(0)$ and $\tilde{R} \geq R(0)$ such that

$$(n+q-2)(2\tilde{R})^{q-2}M - \tilde{\rho} \leq 0, \quad \frac{n+1}{n} \left(\frac{M}{\omega_n} \right)^{1/n} \tilde{\rho}^{1-\frac{1}{n}} - cM\tilde{R}^{q-1} \leq 0. \quad (54)$$

Therefore, the region $[0, \tilde{\rho}] \times [0, \tilde{R}]$ is invariant for the system of differential inequalities (48) and (53) and for any $t \geq 0$, the density ρ and the radius of its support are bounded by $\tilde{\rho}$ and \tilde{R} , respectively.

Existence and uniqueness of the solutions. Reformulate the PDE model (44a)–(44c) in terms of particle-trajectory equations, i.e. system (29a) and (29b) with \mathcal{F} given by

$$\mathcal{F}(X(\alpha, t)) = \int_{\mathbb{R}^n} \left(\frac{1}{n\omega_n} \frac{X(\alpha, t) - X(\beta, t)}{|X(\alpha, t) - X(\beta, t)|^n} - |X(\alpha, t) - X(\beta, t)|^{q-2} (X(\alpha, t) - X(\beta, t)) \right) \times \rho_0(\beta) \, d\beta. \quad (55)$$

Existence and uniqueness of the particle-trajectory system can be studied very similarly to the analysis of the case $q = 2$ from section 2. Using the same setup (Banach space \mathcal{B} , open subset \mathcal{O}_L), one can show the Lipschitz continuity of the map \mathcal{F} and infer local existence and uniqueness. Then, similar to the case $q = 2$, one can use the uniform bound on the density and invoke a Beale–Kato–Majda type argument to extend the result globally in time. The uniform bound on the support of the density is another key ingredient in the estimates. Also needed for global continuation in time is a lower bound on the Jacobian J of the particle map $X(\alpha, t)$. For $q > 2$ we do not have an explicit calculation of the Jacobian $J(\alpha, t)$ as for case $q = 2$, but we can use the differential equation that J satisfies,

$$\frac{d}{dt} J(\alpha, t) = J(\alpha, t) \operatorname{div} v(X(\alpha, t), t),$$

and derive

$$J(\alpha, t) = \exp \left(\int_0^t \operatorname{div} v(X(\alpha, s), s) \, ds \right).$$

Hence, using (45),

$$\begin{aligned} J(\alpha, t) &\geq \exp \left(-(\|\rho\|_{L^\infty} + (n+q-2)(2R)^{q-2}M)t \right) \\ &> \exp \left(-(\tilde{\rho} + (n+q-2)(2\tilde{R})^{q-2}M)t \right). \end{aligned}$$

We summarize these results in the following theorem:

Theorem 3.2 (Global existence and uniqueness for $q > 2$). *Consider the trajectory equations (29a), (29b) and (55) with the Banach space setup and notations from section 2, and a compactly supported initial density $\rho_0 \in L^\infty(\mathbb{R}^n)$, with $|\rho_0|_\gamma < \infty$, for some $\gamma \in (0, 1)$. Then, for every T , there exists $L > 0$ and a unique solution $X \in C^1([0, T]; \mathcal{O}_L)$ to (29a), (29b) and (55) (a unique solution exists globally in time).*

3.2. Radially symmetric steady states

Numerical simulations indicate that the attractors of the dynamics of (44a)–(44c) are always radially symmetric and compactly supported. Guided by this observation, assume the model

(44a)–(44c) admits a radially symmetric steady state $\bar{\rho}(r)$ ⁴ supported on the ball $B(0, R)$. The velocity v is zero in $B(0, R)$, so its divergence also vanishes. Use (45) to find

$$\bar{\rho} - (n + q - 2) \int_{\mathbb{R}^n} |x - y|^{q-2} \bar{\rho}(y) dy = 0 \quad \text{in } B(0, R).$$

Therefore, the density $\bar{\rho}$ satisfies the following homogeneous Fredholm integral equation

$$\bar{\rho}(r) = c(q, n) \int_0^R (r')^{n-1} \bar{\rho}(r') I(r, r') dr', \quad 0 \leq r < R, \quad (56)$$

where

$$c(q, n) = \frac{n(n + q - 2)\omega_n}{\int_0^\pi \sin^{n-2} \theta d\theta}$$

and

$$I(r, r') = \int_0^\pi (r^2 + (r')^2 - 2rr' \cos \theta)^{q/2-1} \sin^{n-2} \theta d\theta.$$

In other words, $\bar{\rho}$ is an eigenfunction of the linear operator T_R , where

$$T_R \bar{\rho}(r) = c(q, n) \int_0^R (r')^{n-1} \bar{\rho}(r') I(r, r') dr', \quad (57)$$

that corresponds to eigenvalue one. Here the subscript is used to emphasize the dependence of the integral operator on the radius R . This eigenvalue problem consists in determining the eigenfunction $\bar{\rho}$ and the radius R of the support. The actual steady density is a constant multiple of this eigenfunction, where the constant is determined from the initial mass.

We state below an existence and uniqueness result regarding the steady states and also present an algorithm for computing them.

Theorem 3.3. *For every $q \geq 2$ and $M > 0$, there exists a unique radius R (that depends on q and n only) and a unique radially symmetric steady state $\bar{\rho}$ of the aggregation model (44a)–(44c) that is supported on $B(0, R)$, has mass M and is continuous on its support.*

Proof. We use a scaling argument and consider the case $R = 1$ first. For $q \geq 2$, since the kernel $c(q, n)(r')^{n-1} I(r, r')$ is nonnegative, continuous and bounded, the corresponding operator T_1 is strongly positive and bounded. We apply the Krein–Rutman theorem [26] to operator T_1 in the following setup. Take the cone in $C([0, 1], \mathbb{R})$ consisting of all non-negative functions. T_1 is a linear, strongly positive, compact operator that maps the space of continuous functions $C([0, 1], \mathbb{R})$ into itself. By Krein–Rutman theorem (see theorem 1.2 in [26]), there exists a positive eigenfunction $\bar{\rho}_1$ such that $T_1 \bar{\rho}_1 = \lambda \bar{\rho}_1$, where λ (which depends only on q and n) is the spectral radius of T_1 . Moreover, the eigenvalue λ is simple and there is no other eigenvalue with a positive eigenvector. By making the change of variable

$$\bar{\rho}(r) = \bar{\rho}_1(r/R) \quad (58)$$

in (57), we obtain

$$T_R \bar{\rho}(r) = R^{n+q-2} \lambda \bar{\rho}(r).$$

Now ask that $\bar{\rho}$ is an eigenfunction of T_R corresponding to eigenvalue one and find

$$R = \lambda^{-\frac{1}{n+q-2}}, \quad (59)$$

⁴ By abuse of notation, we write $\bar{\rho}(r) = \bar{\rho}(x)$.

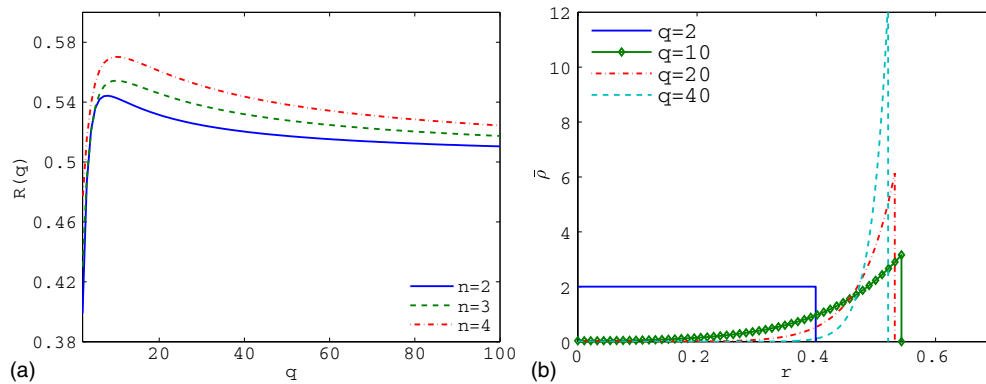


Figure 2. (a) Plot of the radius of the support R of the steady states of (1a), (1b) and (8), as a function of the exponent q , for various space dimensions n . The plot suggests that the radius R approaches asymptotically a constant, as $q \rightarrow \infty$. (b) Normalized radially symmetric steady states $\bar{\rho}(r)$ of (1a), (1b) and (8) in two dimensions for various values of the exponent q . For $q = 2$ the steady state is the constant solution in a disc. As q increases, the qualitative features of the steady states change, as mass aggregates towards the edge of the swarm, creating an increasingly void region in the centre. This suggests that, as $q \rightarrow \infty$, the steady states in two dimensions approach a ring solution of non-zero radius.

which gives the radius of the support as a function of q and n only. Once a mass M for $\bar{\rho}$ is set, uniqueness can be inferred from the uniqueness properties of the spectral radius of T_1 and its associated eigenfunction $\bar{\rho}_1$. \square

This theorem also suggests an algorithm, called the power method [27], to calculate the steady state $\bar{\rho}$. Given an initial positive density $\bar{\rho}^{(0)}$ on $[0, 1]$, consider the iterative scheme

$$\bar{\rho}^{(m+1)} = T_1 \bar{\rho}^{(m)} / \|T_1 \bar{\rho}^{(m)}\|,$$

where $\|\cdot\|$ can be any norm for functions on the unit interval $[0, 1]$. The sequence $\bar{\rho}^{(m)}$ converges to $\bar{\rho}_1$, and the spectral radius of T_1 is given by

$$\lambda = \lim_{m \rightarrow \infty} \|T_1 \bar{\rho}^{(m)}\| / \|\bar{\rho}^{(m)}\|.$$

The steady state $\bar{\rho}$ can then be calculated from (59) and (58).

For numerical purposes we discretize the integral operator T_1 by trapezoidal rule. Using this numerical procedure we first investigate how the radii R of the support of the steady states depend on the exponent q . In figure 2(a) we plot R as a function of q for various values of the space dimension n . The plot suggests that R approaches a constant as $q \rightarrow \infty$, but careful asymptotics will have to support this claim. We plan to investigate this issue in future work.

Figure 2(b) shows the steady state densities $\bar{\rho}(r)$ in two dimensions, corresponding to various values of the exponent q . The plots represent $\bar{\rho}$ as a function of the radial coordinate r . All steady states presented in figure 2(b) are normalized to have unit mass $M = 1$. For $q = 2$ the steady state is the constant solution in a disc. As q increases, the qualitative features of the steady states change: mass aggregates towards the edge of the swarm, creating an increasingly void region in its centre. Combined with the numerical results presented in figure 2(a), figure 2(b) suggests that, as $q \rightarrow \infty$, the steady states in two dimensions approach a ring solution of non-zero radius, similar to equilibria investigated in [28].

In the next paragraph we consider the case when q is even. In this case we are able to determine the precise structure of the steady states. More specifically, we find that for q even the steady states are polynomials of even powers of r .

Case q even (polynomial steady states). When q is an even positive integer, the kernel $I(r, r')$ is separable and the density $\bar{\rho}(r)$ is a polynomial of even powers of r , of degree $q - 2$. To show this, denote by m_i the i th order moments of the density, defined by

$$m_i = n\omega_n \int_0^R r^{n+i-1} \bar{\rho}(r) dr. \quad (60)$$

Note that the zeroth moment m_0 coincides with the total mass M .

When $q = 2$, we recover the steady state investigated in section 2. Indeed,

$$I(r, r') = \int_0^\pi \sin^{n-2} \theta d\theta,$$

and, from (56) and (60),

$$\begin{aligned} \bar{\rho}(r) &= n^2 \omega_n \int_0^R (r')^{n-1} \bar{\rho}(r') dr' \\ &= nm_0. \end{aligned}$$

Using this in the definition of m_0 from (60) yields the identity

$$\begin{aligned} m_0 &= n\omega_n \int_0^R nm_0 r^{n-1} dr \\ &= n\omega_n m_0 R^n. \end{aligned}$$

The last two equations determine the radius of the support $R = (n\omega_n)^{-1/n}$ and the constant density $\bar{\rho} = nm_0$ is determined by the initial mass m_0 . These are the steady states analysed in detail in section 2.

For $q = 4$,

$$I(r, r') = (r^2 + (r')^2) \int_0^\pi \sin^{n-2} \theta d\theta,$$

and

$$\begin{aligned} \bar{\rho}(r) &= n(n+2)\omega_n \int_0^R (r')^{n-1} (r^2 + (r')^2) \bar{\rho}(r') dr' \\ &= (n+2)m_0 r^2 + (n+2)m_2. \end{aligned} \quad (61)$$

The steady state $\bar{\rho}$ is a polynomial of even powers of r , of degree 2, with coefficients given in terms of the moments m_0 and m_2 . We compute R , m_0 and m_2 using the following procedure. Using (61) in the definitions of m_0 and m_2 from (60) we find the linear system

$$\begin{pmatrix} m_0 \\ m_2 \end{pmatrix} = \begin{pmatrix} n\omega_n R^{n+2} & (n+2)\omega_n R^n \\ \frac{n(n+2)}{n+4} \omega_n R^{n+4} & n\omega_n R^{n+2} \end{pmatrix} \begin{pmatrix} m_0 \\ m_2 \end{pmatrix}. \quad (62)$$

The existence of nontrivial solutions for this eigenvalue problem yields a value for the radius R ,

$$R = \left[\omega_n \left(n + (n+2) \sqrt{\frac{n}{n+4}} \right) \right]^{-\frac{1}{n+2}}, \quad (63)$$

and a relation between moments

$$m_2 = \frac{1 - n\omega_n R^{n+2}}{(n+2)\omega_n R^n} m_0. \quad (64)$$

Given an initial mass M , $m_0 = M$ and the steady state can now be found from (61), (63) and (64).

Note that system (62) is equivalent to

$$\begin{pmatrix} m_0 \\ m_2/R^2 \end{pmatrix} = n(n+2)\omega_n R^{n+2} A_{4,n} \begin{pmatrix} m_0 \\ m_2/R^2 \end{pmatrix},$$

where the matrix

$$A_{4,n} = \begin{pmatrix} \frac{1}{n+2} & \frac{1}{n} \\ \frac{1}{n+4} & \frac{1}{n+2} \end{pmatrix}$$

is independent of R .

This pattern extends to arbitrary even q 's. Indeed, from the trinomial expansion of $I(r, r')$, as any odd power of $-rr' \cos \theta$ vanishes, $I(r, r')$ is a polynomial of even powers of r and r' with positive coefficients (note that the moments m_0, \dots, m_{q-2} are positive). Therefore $\bar{\rho}(r)$ is a polynomial of even powers of r , of degree $q - 2$, with positive coefficients, which can be expressed in terms of the moments m_0, \dots, m_{q-2} . Then, the definitions of the moments m_0, m_2, \dots, m_{q-2} yield the system

$$\begin{pmatrix} m_0 \\ m_2/R^2 \\ \vdots \\ m_{q-2}/R^{q-2} \end{pmatrix} = n(n+q-2)\omega_n R^{n+q-2} A_{q,n} \begin{pmatrix} m_0 \\ m_2/R^2 \\ \vdots \\ m_{q-2}/R^{q-2} \end{pmatrix}, \quad (65)$$

where $A_{q,n}$ is a matrix independent of the radius R that has only positive entries.

Apply the Perron–Frobenius theorem [29] to the positive matrix $A_{q,n}$ to conclude that $A_{q,n}$ has an eigenvector with all components positive and that this eigenvector corresponds to the Perron–Frobenius eigenvalue. In addition, the Perron–Frobenius eigenvalue is simple and no other eigenvalue has eigenvectors with only positive components. Since the desired eigenvector in (65) has only positive entries, it has to correspond to the Perron–Frobenius eigenvalue of $A_{q,n}$. Recall that the matrix $A_{q,n}$ does not depend on R , so nor does its Perron–Frobenius eigenvalue. Hence, from (65), one can find R in terms of n and q only. Finally, the steady-state density $\bar{\rho}$ can be found from its polynomial expansion, once a mass $m_0 = M$ is set.

Remark. We want to emphasize that the polynomial states, that correspond to potential (8) with q even, have support of *fixed* (in terms of q and n) radius R . In section 4 we consider an *arbitrary* support radius R , arbitrary radially symmetric densities $\bar{\rho}$ of polynomial form and find an interaction potential for which $\bar{\rho}$ is an equilibrium of the aggregation model (1a) and (1b).

3.3. Dynamic evolution of the aggregation model: numerical results

We compute numerically the solutions to the aggregation model (1a), (1b) and (8), with ϕ given by (7). Several approaches can be taken to discretize the model equation. One is to use its Lagrangian counterpart and evolve numerically the particle trajectories $X_i(t)$, $i = 1, \dots, N$ according to (5). This method is suitable for general initial conditions. However, when initial conditions are radially symmetric, this method is very inefficient in dimension $n \geq 2$ as it does not take advantage of the underlying symmetry. For radially symmetric configurations, we develop below a more suitable method which does take the radial symmetry into account.

The numerical results of this section are obtained from a discretization of the model equations written in characteristic form (see (29a) and (29b), (55) and (46)):

$$\frac{dx}{dt} = \int_{\mathbb{R}^n} \frac{x-y}{n\omega_n|x-y|^n} \rho(y) dy - \int_{\mathbb{R}^n} (x-y)|x-y|^{q-2} \rho(y) dy \quad (66a)$$

$$\frac{d\rho}{dt} = \rho \left[(n+q-2) \int_{\mathbb{R}^n} |x-y|^{q-2} \rho(y) dy - \rho \right]. \quad (66b)$$

Assuming radial symmetry of solutions⁵ we write system (66a) and (66b) as

$$\frac{dr}{dt} = \frac{1}{r^{n-1}} \int_0^r (r')^{n-1} \rho(r') dr' - \omega_{n-1} \int_0^\infty \rho(r') \int_0^\pi (r - r' \cos \theta)(r^2 + r'^2 - 2rr' \cos \theta)^{q/2-1} \sin^{n-2} \theta d\theta dr' \quad (67a)$$

$$\frac{d\rho}{dt} = \rho \left[(n+q-2)\omega_{n-1} \int_0^\infty \rho(r') \int_0^\pi (r^2 + r'^2 - 2rr' \cos \theta)^{q/2-1} \sin^{n-2} \theta d\theta dr' - \rho \right]. \quad (67b)$$

Here the term associated with the singular repulsion in (67a) is calculated by taking advantage of the fact that the corresponding kernel is the fundamental solution of the Laplace equation.

By introducing the following auxiliary functions,

$$I_1(s) = \int_0^\pi (1 - s \cos \theta)(1 + s^2 - 2\rho \cos \theta)^{\gamma/2-1} \sin^{n-2} \theta d\theta, \quad (68a)$$

$$I_2(s) = \int_0^\pi (s - \cos \theta)(1 + s^2 - 2\rho \cos \theta)^{\gamma/2-1} \sin^{n-2} \theta d\theta, \quad (68b)$$

$$I_3(s) = \int_0^\pi (1 + s^2 - 2\rho \cos \theta)^{\gamma/2-1} \sin^{n-2} \theta d\theta, \quad (68c)$$

the angular integrals in θ in (67a) and (67b) become products of powers of r, r' , and these auxiliary functions with $s = \min(r, r')/\max(r, r')$. Hence the double integral in (67a) and (67b) becomes a single integral in r' and is evaluated by trapezoidal rule. This observation reduces the total complexity in the computations of the right-hand-sides of the characteristic equations (67a) and (67b) to $O(N^2)$ per time step where N is the number of spatial grids in r . Once the characteristic speeds in (67a) and (67b) are found, the equations are evolved in time by the classical fourth order Runge–Kutta method.

Figures 3(a) and (b) show simulation results in two dimensions, corresponding to $q = 2$ and $q = 4$, respectively. We plot the solution against the radial coordinate r . The initial data used in figure 3 are

$$\rho(x, 0) = (0.1 - 10|x|^2 + 100|x|^4) \exp(-6|x|^2)/c, \quad (69)$$

where c is a constant chosen to normalize the mass to one. Recall that for both $q = 2$ and $q = 4$ we computed analytically the (unique) radially symmetric steady states. For $q = 2$ the steady density $\bar{\rho}$ is uniform on a disc and zero elsewhere and in section 2.2 we proved that $\bar{\rho}$ attracts all radially symmetric solutions. Further numerical investigations with using random initial conditions (see figure 1) indicate that $\bar{\rho}$ is a *global* attractor for the dynamics of (1a) and (1b), (8), that is, it attracts *all* solutions, not only those that are radially symmetric.

Figure 3(b) shows the time evolution for $q = 4$. An analytic expression of the steady density was calculated in section 3.2. Notice how the solution approaches this steady state and at $t = 16$ is barely indistinguishable from it. Similar behaviours are observed for other exponents $q > 2$ and higher dimensions n . All numerical experiments we performed suggest that the radially symmetric steady states discussed in section 3.2 are global attractors for solutions of (1a), (1b) and (8). In future work to plan to address this issue in an analytical study on the asymptotic dynamics of our aggregation model.

⁵ The method applies only to radially symmetric solutions. However, the claim we make, that the steady states computed in section 3.2 are global attractors, was supported by numerical computations with methods which do not assume radial symmetry, such as the discretization of the ODE particle system (5).

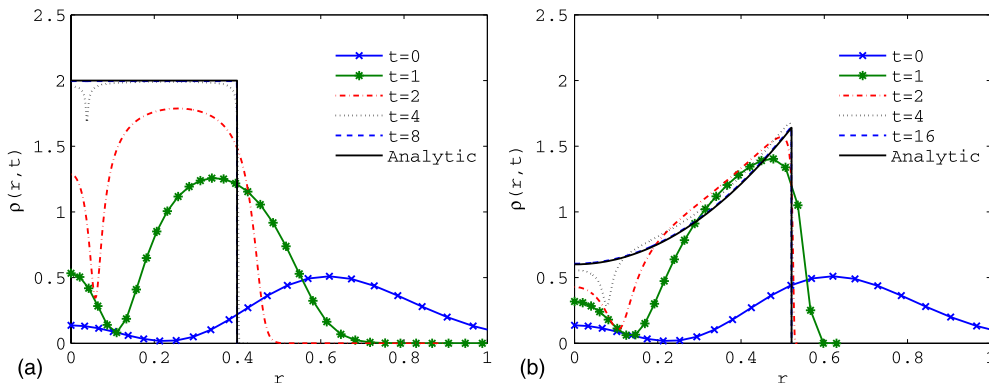


Figure 3. Time evolution of a radially symmetric solution to the aggregation model (1a), (1b) and (8) with (a) $q = 2$ and (b) $q = 4$, in two dimensions, starting from initial data (69). (a) As predicted by the analytical results from section 2, the solution approaches asymptotically a constant, compactly supported steady state. (b) The solution approaches asymptotically the steady state computed analytically in section 3.2—see equations (61), (63) and (64).

4. The inverse problem: custom-designed kernels

We have shown in section 3 that for K of the form (8) with q even, it is possible to construct an explicit procedure for computing the radially symmetric equilibria. It is then natural to consider the following *inverse problem*: given a density $\bar{\rho}(x)$, can we find a kernel for which $\bar{\rho}(x)$ is a steady state of (1a) and (1b)? In this section we show that if $\bar{\rho}(x)$ is radial and is a polynomial in $|x|$, then the answer is always *yes*. Indeed, the construction is a partial generalization of the computations done for the case of even q in section 3. The main results are stated in theorem 4.1 (for $n = 1$) and theorem 4.2 (for $n \geq 2$). Some examples of the construction are also given.

Throughout this section, we use the notation (4) which relates the force F with the radially symmetric potential K . The results below are expressed in terms of $F(r)$.

4.1. One dimension

In one dimension radial symmetry of the steady state is replaced by the requirement that $\bar{\rho}$ is an even function. The result in one dimension is the following.

Theorem 4.1. *In one dimension, consider an even density $\bar{\rho}$ of the form*

$$\bar{\rho}(x) = \begin{cases} b_0 + b_2x^2 + b_4x^4 + \dots + b_{2d}x^{2d} & |x| < R \\ 0 & \text{otherwise.} \end{cases} \quad (70)$$

Define the moments m_i as in (60). Then $\bar{\rho}(x)$ is the steady state of (1a) and (1b) corresponding to the force (see equation (4))

$$F(x) = \frac{1}{2} - \sum_{i=0}^d \frac{a_{2i}}{2i+1} x^{2i+1} \quad (71)$$

where the constants a_0, a_2, \dots, a_{2d} , are computed from b_0, b_2, \dots, b_{2d} by solving the following linear system:

$$b_{2k} = \sum_{j=k}^d a_{2j} \binom{2j}{2k} m_{2(j-k)}, \quad k = 0 \dots d. \quad (72)$$

Moreover, system (72) has a unique solution.

Proof. From (4), we find

$$K(|x|) = - \int_0^{|x|} F(s) ds. \quad (73)$$

Introduce the expression (71) of the force F in the equation above to find

$$K(|x|) = \phi(x) + \sum_{i=0}^d \frac{a_{2i}}{(2i+1)(2i+2)} |x|^{2i+2}.$$

Here, ϕ represents Green's function of $-\frac{d^2}{dx^2}$ defined by (7) (for $n = 1$). Calculate

$$K''(x) = -\delta(x) + H(|x|),$$

where H is given by

$$H(r) = a_0 + a_2 r^2 + \dots + a_{2d} r^{2d}. \quad (74)$$

From (1b),

$$\begin{aligned} \bar{v}'(x) &= -K'' * \bar{\rho} \\ &= \bar{\rho}(x) - \int_{-\infty}^{\infty} H(|x-y|) \bar{\rho}(y) dy. \end{aligned}$$

We want $\bar{\rho}$ given by (70) to be a steady state of (1a) and (1b) corresponding to the force (71). Since $\bar{\rho}$ is zero outside the interval $|x| < R$, the velocity \bar{v} has to vanish inside the interval. In particular, $\bar{v}' = 0$ in $|x| < R$, and the steady state $\bar{\rho}$ satisfies the integral equation:

$$\bar{\rho}(x) = \int_{-\infty}^{\infty} H(|x-y|) \bar{\rho}(y) dy \quad \text{in } |x| < R. \quad (75)$$

Calculate using the binomial expansion,

$$\begin{aligned} \int_{-\infty}^{\infty} |x-y|^{2j} \bar{\rho}(y) dy &= 2 \int_0^R \sum_{k=0}^j y^{2(j-k)} x^{2k} \binom{2j}{2k} \bar{\rho}(y) dy \\ &= \sum_{k=0}^j x^{2k} \binom{2j}{2k} m_{2(j-k)}. \end{aligned}$$

Here we also used definition (60) and the fact that $\bar{\rho}$ vanishes outside $|x| < R$. The integral equation (75) now becomes

$$\begin{aligned} \bar{\rho}(x) &= \sum_{j=0}^d a_{2j} \sum_{k=0}^j x^{2k} \binom{2j}{2k} m_{2(j-k)} \\ &= \sum_{k=0}^d x^{2k} \left[\sum_{j=k}^d \binom{2j}{2k} m_{2(j-k)} a_{2j} \right] \quad \text{in } |x| < R. \end{aligned}$$

By equating the coefficients in $\bar{\rho}(x)$ from the equation above with those from the expression (70) we find (72). This is a linear system to be solved for coefficients a_0, a_2, \dots, a_{2d} in terms of b_0, b_2, \dots, b_{2d} . The existence and uniqueness of a solution is immediate since (72) is a triangular linear system with non-zeros along the diagonal, since $m_0 = M \neq 0$. \square

We illustrate theorem 4.1 with three examples. We take $R = 1$ and consider

$$(a) \bar{\rho}(x) = 1 - x^2; \quad (b) \bar{\rho}(x) = x^2; \quad (c) \bar{\rho}(x) = \frac{1}{2} + x^2 - x^4, \quad (76)$$

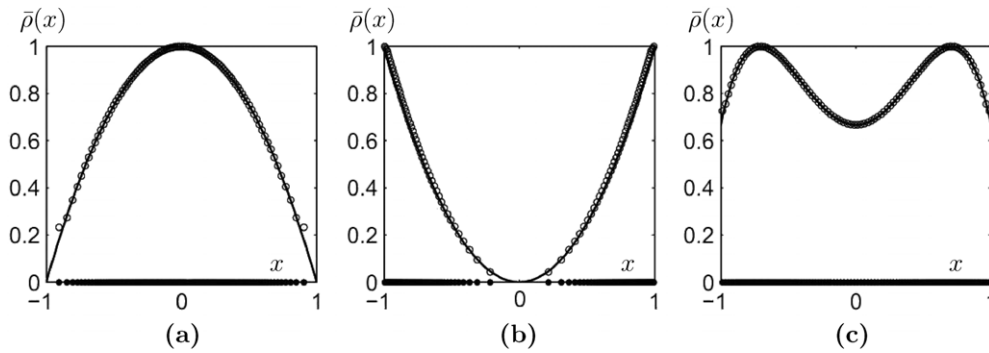


Figure 4. (a)–(c) Steady state solutions to (1a) and (1b) in one dimension with force $F(x)$ given by (77). Filled circles along the x -axis represent the steady state for the corresponding dynamical system (5) with $N = 50$ particles. Empty circles represent the density function as computed from the filled circles, normalized so that $\max \bar{\rho} = 1$. The solid line is the analytical expression for $\bar{\rho}$ given by (76), but normalized so that $\max \bar{\rho} = 1$. In all cases, excellent agreement is observed between the asymptotic behaviour and the predicted steady states.

which represent a convex, a concave, and a two-bumped steady state, respectively. From theorem 4.1, the corresponding forces are given by

$$\begin{aligned}
 (a) \quad F(x) &= \frac{1}{2} - \frac{9}{10}x + \frac{1}{4}x^3; & (b) \quad F(x) &= \frac{1}{2} + \frac{9}{10}x - \frac{1}{2}x^3; \\
 (c) \quad F(x) &= \frac{1}{2} + \frac{209425}{672182}x - \frac{2075}{2527}x^3 + \frac{3}{19}x^5. & & (77)
 \end{aligned}$$

In figure 4 we plot $\bar{\rho}(r)$ as given by (76) (solid lines), as well as the numerically computed equilibria obtained by evolving in time solutions of the aggregation model corresponding to forces (77) (empty circles). To evolve the aggregation model numerically we used a discretization of the ODE particle system (5) with $N = 50$ particles, starting from random initial conditions in $[-1, 1]$. The system was integrated using Euler method with stepsize 0.1 until $t = 5000$, by which point the system settled to the equilibrium state. The approximated continuum density $\bar{\rho}(x)$ was computed using the procedure described in [8]. Note the excellent agreement observed in all cases.

The computations of this section can be generalized to some non-polynomial steady states $\bar{\rho}$. For example if $\bar{\rho}$ has a convergent Taylor series on $[0, R]$, one can approximate $\bar{\rho}$ by its truncated Taylor series of degree $2d$, apply theorem 4.1, and then take the limit $d \rightarrow \infty$. Alternatively, the integral equation (75) can sometimes be used directly to determine the corresponding force F . To illustrate this, consider

$$\bar{\rho}(x) = \cos x, \quad R = \pi/2, \quad (78)$$

so that (75) becomes

$$\cos x = \int_{-\pi/2}^{\pi/2} H(|x - y|) \cos y \, dy. \quad (79)$$

Using the ansatz $H(z) = a + b \cos z$, we find that (79) is satisfied for all x when $a = 0$ and $b = 2/\pi$. Therefore $H(x) = 2/\pi \cos x$ and

$$F(x) = 1/2 - 2/\pi \sin x. \quad (80)$$

Direct integration of the ODE system (5) using the force (80) confirms that the model admits indeed the steady state given by (78).

4.2. Higher dimensions

The construction in higher dimensions is analogous to 1D. We state the result only for $n = 2$ and $n = 3$, but the procedure generalizes easily to any dimension n .

Theorem 4.2. *In dimension $n = 2$ or $n = 3$, consider a radially symmetric density $\bar{\rho}(x) = \bar{\rho}(|x|)$ of the form*

$$\bar{\rho}(r) = \begin{cases} b_0 + b_2 r^2 + b_4 r^4 + \dots + b_{2d} r^{2d} & |x| < R \\ 0 & \text{otherwise.} \end{cases} \quad (81)$$

Define the moments m_i as in (60). Then $\bar{\rho}(r)$ is the steady state of (1a) and (1b) corresponding to the force (see equation (4))

$$F(r) = \frac{1}{n\omega_n} \frac{1}{r^{n-1}} - \sum_{i=0}^d \frac{a_{2i}}{2i+n} r^{2i+1}, \quad (82)$$

where the constants a_0, a_2, \dots, a_{2d} are computed from b_0, b_2, \dots, b_{2d} by solving the following linear system:

$$b_{2k} = \sum_{j=k}^d a_{2j} C_{n,j,k} m_{2(j-k)}, \quad k = 0 \dots d, \quad (83)$$

with

$$C_{n,j,k} = \begin{cases} \binom{j}{k}^2, & n = 2 \\ \frac{1}{2(j+1)} \binom{2(j+1)}{2k+1}, & n = 3. \end{cases} \quad (84)$$

Moreover, system (83) has a unique solution.

Proof. The proof follows closely the argument from the one-dimensional case. From (73), we find, using the expression (82) for the force F :

$$K(|x|) = \phi(x) + \sum_{i=0}^d \frac{a_{2i}}{(2i+n)(2i+2)} |x|^{2i+2}. \quad (85)$$

Here, ϕ represents Green's function of $-\Delta$ in \mathbb{R}^n , defined by (7)⁶. Calculate

$$\Delta K(x) = -\delta(x) + H(|x|),$$

where H is given by (74). Calculate from (1b):

$$\begin{aligned} \nabla \cdot \bar{v}(x) &= -\Delta K * \bar{\rho}(x) \\ &= \bar{\rho}(x) - \int H(|x-y|) \bar{\rho}(y) dy. \end{aligned}$$

The steady state $\bar{\rho}$ from (81) must have zero velocity in the ball $|x| < R$, hence $\bar{\rho}$ satisfies the integral equation:

$$\bar{\rho}(x) = \int H(|x-y|) \bar{\rho}(y) dy \quad \text{in } |x| < R. \quad (86)$$

⁶ The potentials of the form (85) include the family of potentials (8) with q even. To see this, take $2d+2 = q$, $a_{2d} \neq 0$ and $a_{2i} = 0$ for all $0 \leq i < d$.

From radial symmetry $\bar{\rho}(y) = \bar{\rho}(|y|)$, we have

$$\int_{\mathbb{R}^n} |x - y|^{2j} \bar{\rho}(y) \, dy = \left(\frac{n\omega_n}{\int_0^\pi \sin^{n-2} \theta \, d\theta} \right) \int_0^\infty \left(\int_0^\pi (s^2 + r^2 - 2rs \cos \theta)^j \sin^{n-2} \theta \, d\theta \right) \\ \times \bar{\rho}(r) r^{n-1} \, dr,$$

where $s = |x|$. Next we simplify as follows:

$$\frac{1}{\int_0^\pi \sin^{n-2} \theta \, d\theta} \int_0^\pi (s^2 + r^2 - 2rs \cos \theta)^j \sin^{n-2} \theta \, d\theta = Q_{n,2j}(s/r) r^{2j}$$

where we define

$$Q_{n,2j}(t) := \frac{1}{\int_0^\pi \sin^{n-2} \theta \, d\theta} \int_0^\pi (t^2 + 1 - 2t \cos \theta)^j \sin^{n-2} \theta \, d\theta. \quad (87)$$

From (87) it is easy to see that the polynomial $Q_{n,2j}$ of degree $2j$ contains only even powers, so that we may write

$$Q_{n,2j}(t) = \sum_{k=0}^j C_{n,j,k} t^{2k}. \quad (88)$$

In terms of the coefficients $C_{n,j,k}$ we then obtain

$$\int_{\mathbb{R}^n} |x - y|^{2j} \bar{\rho}(y) \, dy = n\omega_n \int_0^\infty \sum_{k=0}^j C_{n,j,k} s^{2k} r^{2(j-k)+n-1} \bar{\rho}(r) \, dr \\ = \sum_{k=0}^j C_{n,j,k} m_{2(j-k)} s^{2k}.$$

We therefore obtain from (86),

$$\bar{\rho}(r) = \sum_{j=0}^d a_{2j} \sum_{k=0}^j C_{n,j,k} m_{2(j-k)} r^{2k} \\ = \sum_{k=0}^d r^{2k} \left[\sum_{j=k}^d C_{n,j,k} m_{2(j-k)} a_{2j} \right] \quad \text{in } |x| < R.$$

Now match with the coefficients of $\bar{\rho}$ from (81) to find (83). The linear system (83) has a unique solution, since the matrix is triangular and its main diagonal has non-zero entries ($m_0 \neq 0$). It remains to show (84). In the two-dimensional case, we expand

$$Q_{2,2j}(t) = \frac{1}{\pi} \int_0^\pi (1 + t^2 - 2t \cos \theta)^j \, d\theta \\ = \frac{1}{\pi} \sum_{i=0}^j \sum_{k=0}^{j-i} \frac{j!}{i!k!(j-i-k)!} t^{2i+k} (-2)^k \int_0^\pi \cos^k \theta \, d\theta.$$

For the integral we have

$$\frac{1}{\pi} \int_0^\pi \cos^k \theta \, d\theta = \begin{cases} 0, & k \text{ is odd} \\ \frac{k!}{2^k \left[\left(\frac{k}{2} \right)! \right]}, & k \text{ is even.} \end{cases}$$

Therefore

$$\begin{aligned}
 Q_{2,2j}(t) &= \frac{1}{2\pi} \sum_{i=0}^j \sum_{k=0}^{\lfloor (j-i)/2 \rfloor} \frac{j!}{i!(2k)!(j-i-2k)!} t^{2i+2k} (-2)^{2k} \int_0^{2\pi} \cos^{2k} \theta \, d\theta \\
 &= \sum_{i=0}^j \sum_{k=0}^{\lfloor (j-i)/2 \rfloor} \frac{j!}{i!(k!)^2(j-i-2k)!} t^{2k+2i}.
 \end{aligned} \tag{89}$$

For $l \leq \lfloor j/2 \rfloor$, the coefficient of t^{2l} is

$$\sum_{i=0}^l \frac{j!}{i!((l-i)!)^2(j-2l+i)!} = \binom{j}{l} \sum_{i=0}^l \binom{j}{i} \binom{j-l}{l-i} = \binom{j}{l}^2. \tag{90}$$

In the last step, we used the combinatoric identity

$$\sum_{i=0}^l \binom{j}{i} \binom{j-l}{l-i} = \binom{j}{l}. \tag{91}$$

This proves (84) with $n = 2$. The case $n = 3$ is much simpler as $Q_{3,2j}(t)$ can be integrated explicitly for general j :

$$\begin{aligned}
 Q_{3,2j}(t) &= \frac{1}{2} \int_0^\pi (1+t^2-2t \cos \theta)^j \sin \theta \, d\theta = \frac{1}{4t} \int_{(1-t)^2}^{(1+t)^2} u^j \, du \\
 &= \frac{1}{4t} \frac{1}{j+1} [(1+t)^{2j+1} - (1-t)^{2j+1}]
 \end{aligned}$$

which leads to (84) with $n = 3$ after some algebra. □

Finally, we illustrate theorem 4.2 with two examples in $n = 2$ dimensions:

$$(a) \bar{\rho}(r) = 1; \quad (b) \bar{\rho}(r) = 1 + r^2. \tag{92}$$

According to theorem 4.2, density (a) in (92) corresponds to the force

$$(a) F(r) = \frac{1}{2\pi} \frac{1}{r} - \frac{1}{2\pi R^2} r.$$

Case $R = 1/\sqrt{2\pi}$, corresponding to the potential (8) with $q = 2$, was considered in section 2.2. For $R = 1$, $F(r) = \frac{1}{2\pi}(\frac{1}{r} - r)$. Multiplying the force F by a constant does not effect the equilibrium solution, as the constant can be removed by rescaling time. The dynamics corresponding to $F(r) = \frac{1}{r} - r$ was presented in figure 1 in the introduction. Indeed, a constant equilibrium on a unit disc is reached.

Corresponding to density (b) in (92) we have, according to theorem 4.2:

$$(b) F(r) = \frac{1}{2\pi} \frac{1}{r} - \frac{4}{27\pi} r - \frac{1}{6\pi} r^3.$$

Example (b) is illustrated in figure 5. The results show an excellent agreement between the predicted steady state of (1a) and (1b) and the asymptotic dynamics of the particle system.

5. Discussion

We have presented several new steady solutions to the aggregation equations (1a) and (1b), in particular for two or higher dimensions. One of the key features of the potential (8) is that the repulsion is proportional to a Newtonian potential. This property was critical for being able to construct the steady states explicitly. In [8] the steady state for the Morse function

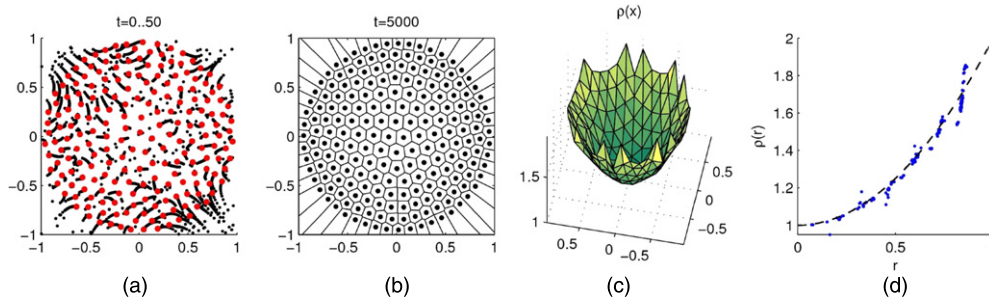


Figure 5. Numerical simulation of (5) in two dimensions with the custom-designed force $F(r) = \frac{1}{2\pi} \frac{1}{r} - \frac{4}{27\pi} r - \frac{1}{6\pi} r^3$, corresponding to the equilibrium density $\bar{\rho}(r) = 1 + r^2$ of (1a) and (1b) (see theorem 4.2). (a) Evolution of $N = 200$ particles with $t = 0 \dots 50$, starting with random initial conditions uniformly distributed inside a unit square. (b) Snapshot of the solution at $t = 5000$. Dots represent the particle positions; lines represent the boundaries of the corresponding Voronoi cells. (c) Estimate of the density $\bar{\rho}(x)$. Delaunay triangulation based on the Voronoi diagram is shown. The density at x_j is $\bar{\rho}(x_j) = 1/a_j$ where a_j is the area of the Voronoi cell around x_j . (d) The scatter plot of the approximated density $\bar{\rho}(x_j)$ versus $|x_j|$ for each particle x_j . Dashed line is the analytical solution $\bar{\rho}(r) = 1 + r^2$.

$F(r) = e^{-r} - Ge^{-r/L}$ was computed analytically in one dimension. It is an open question to generalize this calculation to higher dimensions. In two dimensions, the Morse potential has a much weaker repulsion at the origin ($F(r) = O(1)$ as $r \rightarrow 0$) than the Newtonian potential ($F(r) = O(1/r)$ as $r \rightarrow 0$). For this reason, it is unclear whether the ideas presented here or in [8] can be used to determine the steady states of the Morse function in two dimensions.

For the simple case when the attraction component of the potential is quadratic (K given by (8) with $q = 2$ or alternatively, force F given by (6)), we have proved that the density given by the characteristic function of a ball is a global attractor for radially symmetric initial conditions. However, numerics strongly suggests that this is true for all initial conditions (see for example figure 1). It is an open problem to prove this. A related issue is that the characteristic function of a ball is *not* the unique radially symmetric equilibrium solution that corresponds to force (6). For example, in two dimensions, there exists an equilibrium solution for which the density concentrates on a delta ring whose radius r_0 satisfies (see [28])

$$\int_0^{\pi/2} F(2r_0 \sin(\theta)) \sin(\theta) d\theta = 0.$$

In particular, for $F(r) = 1/r - r$ in two dimensions, we obtain $r_0 = 1/\sqrt{2}$ (whereas the global attractor is the density that is uniform inside a unit disc). However, as was shown in [28], such delta-ring solution is *ill-posed* whenever $F(r) \sim 1/r$ as $r \rightarrow 0$, in the sense that it is unstable with respect to all sufficiently high Fourier modes.

For the more general potential (8) with $q > 2$, we have shown that there exists a unique, bounded and compactly supported radially symmetric equilibrium density. Numerical experiments suggest that these equilibria are global attractors for the dynamics, but a proof is lacking. Another interesting question is what happens when $q < 2$, the regime where the estimates of section 3 are no longer valid. Numerical simulations indicate the existence of concave steady states in this case. These are subjects of future work.

We also solved the restricted inverse problem: given a radially symmetric polynomial density, we explicitly construct a corresponding force which admits the given density as its equilibrium state. However, nothing is known about the stability of such steady states and in

fact they are not generally expected to be globally stable. It would be interesting to provide extra conditions to guarantee the stability of these states.

In a biological setting, stochastic noise often needs to be taken into account. As derived for example in [3, 4] (see also [30, 31] and references therein), this noise can be modelled by adding a diffusion term so that the continuous model (1a) becomes

$$\rho_t + \nabla \cdot (\rho v) = D \Delta \rho, \quad (93)$$

where D represents the noise strength. We expect that for sufficiently small D , the effect of the diffusion is to smooth out the edges of the swarm, without having a large effect on the interior of the swarm. Some of the related results in one dimension are derived in [3, 4]. The proper study of (93) in higher dimensions is left for future work.

The interaction force (6) does not decay at infinity—a biological absurdity. However, the dynamics remain unchanged if $F(r)$ is modified in an arbitrary way for $r > r_1$, where r_1 is some sufficiently large number that depends on the initial conditions⁷. This can be seen from the ODE formulation (5): the velocity $X'_i(t)$ of each particle only depends on $F(r)$ with $r \leq \max_{i,j} |X_i - X_j|$. Moreover, as was shown in section 3, the radius of the support of the density $\rho(x, t)$ is bounded by \tilde{R} where \tilde{R} is given implicitly by (54) and depends only on the initial conditions and not on time. In particular, $F(r)$ can be taken to be zero (or exponentially decreasing) for $r > 2\tilde{R}$, without changing the dynamics. Moreover \tilde{R} can be taken to be R , the radius of the steady state, without changing the structure of the steady state or its local stability. The interaction force (6) is also unbounded at the origin in two (or higher) dimensions, also a biological absurdity. However, within a biological context, where the population size N is finite, one can again truncate $F(r)$ for $r < r_0$ where $r_0 \leq \min_{i \neq j} |X_i - X_j| = O(N^{-1/2})$. This is because for a uniformly distributed steady state of an $O(1)$ radius, the inter-particle distance is at least $O(N^{-1/2})$, so $F(r)$ can be taken to be arbitrary for $r < r_0$ without changing the structure or local stability of the steady state.

To illustrate this, consider the following truncated force in two dimensions,

$$F(r) = \begin{cases} C_1, & 0 \leq r < r_0 \\ \frac{1}{r} - r, & r_0 \leq r \leq 2 \\ -C_2 \exp(-r), & 2 < r \end{cases} \quad (94)$$

where the constants C_1, C_2 are chosen to make $F(r)$ continuous; the truncation point $r_1 = 2$ is chosen to be twice the radius of the steady state of the untruncated force $F(r) = 1/r - r$. The simulation of the ODE system (5) in two dimensions with $N = 400$ is shown in figure 6 for various values of r_0 . Initial conditions were chosen at random inside the unit square. For $r_0 < 0.09$, the steady state is the same as taking $r_0 = 0$. On the other hand, as r_0 is increased further but still small, intricate grid defects are observed, such as concentric rings and irregular tessellations, while the overall swarm radius and density remain roughly the same. The analysis of these defects is an interesting open problem. Finally for $r_0 > 0.2$, the uniformity of the swarm breaks down leading to a very different steady state.

Uniform swarms are often observed in biology; however, the precise mechanisms of their formation are rarely known (but see a recent study [32] which attempts to establish some of these mechanisms through empirical measurements). Regardless, possible biological advantages of uniform swarms may be avoidance of overcrowding and uniform resource distribution among the swarm. We have shown *mathematically* that the model (1a) and (1b) with the force (6) (or its regularizations such as (94)) leads to the formation of such uniform swarms. However, a

⁷ The well-known Keller–Segel model for chemotaxis requires similar cutoffs of the chemotactic function in order to avoid the unphysical blow-up in finite time of the solution [23].

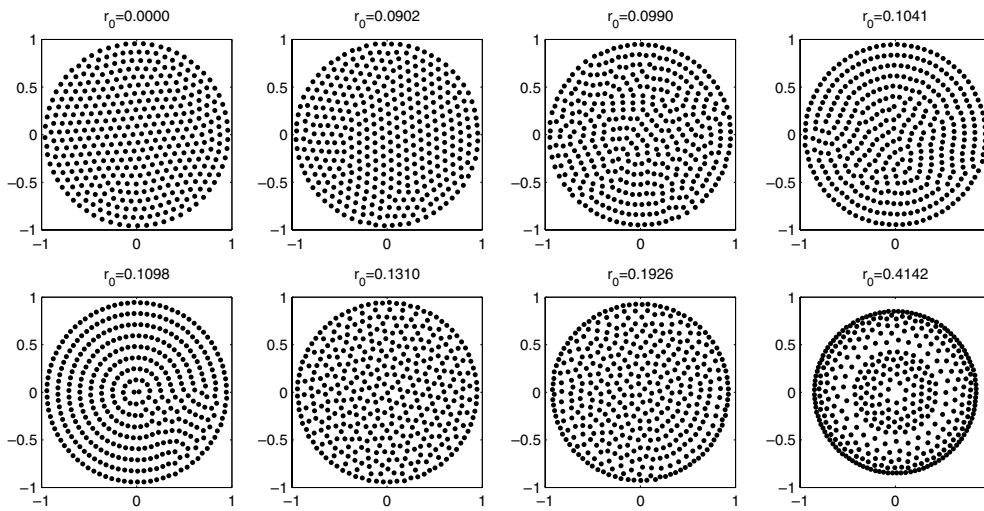


Figure 6. Equilibrium states for the truncated interaction force (94) with $N = 400$. The equilibrium is computed by integrating the ODE system (5) to $t = 5000$, starting from random initial conditions in the unit square. For $r_0 < 0.09$, the steady state is the same as for $r_0 = 0$ (uniform density in the unit circle). As r_0 is increased further, intricate grid defects are observed, while the overall swarm radius and density remain roughly the same. Finally, for $r_0 > 0.2$, the uniformity of the swarm breaks down leading to a very different steady state.

better understanding of the underlying biological mechanisms is needed before any conclusions about the applicability of this model to biology can be made.

Acknowledgments

RF is supported by NSERC discovery grant RGPIN-315973. TK is supported by NSERC discovery grant 47050. We thank the anonymous referees for their careful reading and insightful comments.

Appendix

Proof of theorem 2.1. We present an outline of the proof and refer for details and complete calculations to proposition 4.2, chapter 1 in [24].

First show that the operator $\mathcal{F} : \mathcal{O}_L \rightarrow \mathcal{B}$ is bounded, i.e. $\|\mathcal{F}(X)\|_{1,\gamma} < \infty$, for all $X \in \mathcal{O}_L$. Write $F(X)$ as

$$F(X) = v \circ X.$$

To bound $\|F(X)\|_{1,\gamma}$ we need the following two results from [24], stated in lemmas 4.1 and 4.3, chapter 4:

- (i) Let $X, Y : \mathbb{R}^n \rightarrow \mathbb{R}^n$ be smooth, bounded functions. Then, for $\gamma \in (0, 1]$,

$$|XY|_\gamma \leq \|X\|_{L^\infty} |Y|_\gamma + |X|_\gamma \|Y\|_{L^\infty}. \tag{95}$$

- (ii) Let $X : \mathbb{R}^n \rightarrow \mathbb{R}^n$ be an invertible transformation with $\det \nabla_\alpha X(\alpha) \geq c > 0$, and let $f : \mathbb{R}^n \rightarrow \mathbb{R}^m$ be a smooth function. Then

$$|f \circ X|_\gamma \leq |f|_\gamma \|\nabla_\alpha X\|_{L^\infty}^\gamma. \tag{96}$$

Using these two calculus results one can estimate:

$$\begin{aligned} \|F(X)\|_{1,\gamma} &= |v * X(0)| + \|(\nabla v \circ X)\nabla_\alpha X\|_{L^\infty} + |(\nabla v \circ X)\nabla_\alpha X|_\gamma \\ &\leq \|v\|_{L^\infty} + \|\nabla v\|_{L^\infty}\|X\|_{1,\gamma} + |\nabla v|_\gamma\|\nabla_\alpha X\|_{L^\infty}^{\gamma+1}. \end{aligned} \quad (97)$$

As $\|X\|_{1,\gamma} \leq L$ for $X \in \mathcal{O}_L$, it remains to bound $\|v\|_{L^\infty}$, $\|\nabla v\|_{L^\infty}$ and $|\nabla v|_\gamma$.

The expression (17) for $v(x)$ has two components: the convolution of the singular kernel k with ρ , and $-Mx$. The latter term, due to attraction, presents no difficulties, so we focus on the repulsion component only. The gradient of the repulsion term yields a principal-value SIO that involves the convolution of $P = \nabla k$ with ρ :

$$P[\rho](x) = \text{PV} \int_{\mathbb{R}^2} P(x-y)\rho(y) dy. \quad (98)$$

We have to estimate $\|k * \rho\|_{L^\infty}$, $\|P[\rho]\|_{L^\infty}$ and $|P[\rho]|_\gamma$.

The first of these terms can be bounded using lemma 4.5 [24]:

$$\|k * \rho\|_{L^\infty} \leq C\sqrt{R}\|\rho\|_{L^\infty}, \quad (99)$$

where c is a constant and R is the radius of the support of ρ . Normally R depends on $\|\nabla_\alpha X\|_{L^\infty}$ and is bounded for $X \in \mathcal{O}_L$, but in our problem we have the stronger result that the support is uniformly bounded in time.

To bound the other two terms we use lemma 4.6 (chapter 4 [24]) and estimate

$$\|P[\rho]\|_{L^\infty} \leq c(|\rho|_\gamma \epsilon^\gamma + \|\rho\|_{L^\infty} \log(R/\epsilon)), \quad \forall \epsilon > 0, \quad (100a)$$

$$|P[\rho]|_\gamma \leq c|\rho|_\gamma, \quad (100b)$$

where c represent constants and R relates to the size of the support, as above.

Inspect (99), (100a) and (100b). Given that $\|\rho\|_{L^\infty}$ and R are uniformly bounded in time, it remains to estimate the seminorm $|\rho|_\gamma$. Use (24) and calculus inequality (95) to obtain:

$$|\rho|_\gamma \leq \|\rho_0 \circ X^{-1}\|_{L^\infty} |\det \nabla_x X^{-1}|_\gamma + |\rho_0 \circ X^{-1}|_\gamma \|\det \nabla_x X^{-1}\|_{L^\infty}. \quad (101)$$

The following calculus inequality is stated in lemma 4.2 [24] (n is the space dimension):

$$\|Y^{-1}\|_{1,\gamma} \leq c\|Y\|_{1,\gamma}^{2n-1}, \quad (102)$$

Use (96) and (102) with $n = 2$ to estimate

$$\begin{aligned} |\rho_0 \circ X^{-1}|_\gamma &\leq |\rho_0|_\gamma \|\nabla_x X^{-1}\|_{L^\infty}^\gamma \\ &\leq c|\rho_0|_\gamma \|X\|_{1,\gamma}^{3\gamma}, \end{aligned}$$

and

$$|\det \nabla_x X^{-1}|_\gamma \leq c\|X\|_{1,\gamma}^3.$$

As $X \in \mathcal{O}_L$, $\|\det \nabla_x X^{-1}\|_{L^\infty} < L$ and $\|X\|_{1,\gamma} < L$. Return to (101) to find

$$|\rho|_\gamma \leq C(L) (\|\rho_0\|_{L^\infty} + |\rho_0|_\gamma).$$

Using the above bound on $|\rho|_\gamma$ and the uniform bounds on $\|\rho\|_{L^\infty}$ and R , we infer from (99), (100a) and (100b) that the repulsion component of \mathcal{F} yields a bounded operator. The attraction component is regular and trivial to deal with. We conclude that \mathcal{F} is bounded.

To prove that \mathcal{F} is Lipschitz continuous, we show that $\mathcal{F}'(X)$ is bounded as a linear operator from \mathcal{O}_L to \mathcal{B} , i.e. $\|\mathcal{F}'(X)\| < \infty$, for all $X \in \mathcal{O}_L$. Calculate $\mathcal{F}'(X)$ using (55) and (12c):

$$\begin{aligned} \mathcal{F}'(X)Y &= \left. \frac{d}{d\epsilon} \mathcal{F}(X + \epsilon Y) \right|_{\epsilon=0} \\ &= \int \nabla f(X(\alpha) - X(\beta))(Y(\alpha) - Y(\beta))\rho_0(\beta) d\beta, \end{aligned} \tag{103}$$

where we suppressed the time dependence for convenience.

To estimate the component of $\mathcal{F}'(X)Y$ due to repulsion one could follow the proof of lemma 4.10 in [24]. The attraction component is trivial. It can be shown that

$$\|\mathcal{F}'(X)Y\|_{1,\gamma} \leq C(L) (\|\rho_0\|_{L^\infty} + |\rho_0|_\gamma) \|Y\|_{1,\gamma},$$

which proves the boundedness in the operator norm of $\mathcal{F}'(X)$.

A key observation is that the term $Y(\alpha) - Y(\beta)$ in (103) compensates for the singularity of ∇f . To illustrate this point, we present here the estimate of $\|\mathcal{F}'(X)Y\|_{L^\infty}$. We do not present the estimates of $\|\nabla_\alpha \mathcal{F}'(X)Y\|_{L^\infty}$ and $|\nabla_\alpha \mathcal{F}'(X)Y|_\gamma$, we refer instead to the calculations in [24].

Use a change of variable, $x = X(\alpha)$, $y = X(\beta)$, and split the repulsion component of $\mathcal{F}'(X)Y$ from (103)

$$\int \nabla k(x - y)(Y(X^{-1}(x)) - Y(X^{-1}(y)))\rho(y) dy = \underbrace{\int_{|x-y|<1}}_{J_1} + \underbrace{\int_{|x-y|>1}}_{J_2}.$$

From the mean-value theorem, we have

$$|Y(X^{-1}(x)) - Y(X^{-1}(y))| \leq \|(\nabla_\alpha Y \circ X^{-1})\nabla_x X^{-1}\|_{L^\infty} |x - y|.$$

As $|\nabla k(x)| \leq c|x|^{-2}$,

$$\begin{aligned} |J_1| &\leq c\|(\nabla_\alpha Y \circ X^{-1})\nabla_x X^{-1}\|_{L^\infty} \|\rho\|_{L^\infty} \int_{|x-y|<1} \frac{1}{|x - y|} dy \\ &\leq C(L)\|\nabla_\alpha Y\|_{L^\infty}, \end{aligned}$$

where we also used (102), $X \in \mathcal{O}_L$, and the uniform bound on $\|\rho\|_{L^\infty}$ in the second inequality.

The outer integral satisfies

$$\begin{aligned} |J_2| &\leq c\|(\nabla_\alpha Y \circ X^{-1})\nabla_x X^{-1}\|_{L^\infty} \int_{|x-y|>1} \rho(y) dy \\ &\leq C(L)M\|\nabla_\alpha Y\|_{L^\infty}, \end{aligned}$$

where we used conservation of mass.

Combine the two estimates for J_1 and J_2 . The attraction component would not break these estimates, hence

$$\|\mathcal{F}'(X)Y\|_{L^\infty} \leq C(L)\|Y\|_{1,\gamma}.$$

Proof of proposition 2.3. Take the gradient with respect to α of the characteristic equation (20) to obtain

$$\frac{d}{dt} \nabla_\alpha X(\alpha, t) = \nabla v(X(\alpha, t), t) \nabla_\alpha X(\alpha, t). \tag{104}$$

From (104), one can derive using Gronwall's lemma (also use $X(\alpha, 0) = \alpha$):

$$\|\nabla_\alpha X(\cdot, t)\|_{L^\infty} \leq e^{\int_0^t \|\nabla v(\cdot, s)\|_{L^\infty} ds}. \tag{105}$$

To bound $|\nabla_\alpha X(\cdot, t)|_\gamma$ we use calculus inequalities (95) and (96). Using these two calculus results one can estimate:

$$|\nabla v(X(\cdot, t), t)\nabla_\alpha X(\cdot, t)|_\gamma \leq |\nabla v(\cdot, t)|_\gamma \|\nabla_\alpha X(\cdot, t)\|_{L^\infty}^{1+\gamma} + \|\nabla v(\cdot, t)\|_{L^\infty} |\nabla_\alpha X(\cdot, t)|_\gamma. \tag{106}$$

As noted above, the expression (17) for $v(x)$ has two components: the convolution of the singular kernel k with ρ , and $-Mx$. The gradient of the second component yields $-MI_d$, where I_d denotes the identity matrix. The gradient of the first component yields a principal-value SIO that involves the convolution of $P = \nabla k$ with ρ —see (98).

Use lemma 4.6 (chapter 4 [24]) and estimate the γ -seminorm of $P[\rho]$:

$$|P[\rho]|_\gamma \leq c(\|\rho\|_{L^\infty} + |\rho|_\gamma),$$

where c is a constant. Note that this result holds for functions of uniform compact support, condition which the solution ρ does indeed satisfy. Collect the terms that comprise ∇v and use the uniform bound (23) on $\|\rho\|_{L^\infty}$ to find

$$|\nabla v(\cdot, t)|_\gamma \leq C(1 + |\rho(\cdot, t)|_\gamma).$$

Using this estimate and (105) in (106), we derive

$$|\nabla v(X(\cdot, t), t)\nabla_\alpha X(\cdot, t)|_\gamma \leq C(1 + |\rho(\cdot, t)|_\gamma) e^{(1+\gamma) \int_0^t \|\nabla v(\cdot, s)\|_{L^\infty} ds} + \|\nabla v(\cdot, t)\|_{L^\infty} |\nabla_\alpha X(\cdot, t)|_\gamma.$$

Below we estimate the term $|\rho(\cdot, t)|_\gamma$ in terms of $\int_0^t \|v(\cdot, s)\|_{L^\infty} ds$ and show

$$|\rho(\cdot, t)|_\gamma \leq |\rho_0|_\gamma e^{C_1 t} \exp \left[\gamma \int_0^t \|\nabla v(\cdot, s)\|_{L^\infty} ds \right]. \tag{107}$$

Hence,

$$|\nabla v(X(\cdot, t), t)\nabla_\alpha X(\cdot, t)|_\gamma \leq C(1 + |\rho_0|_\gamma e^{C_1 t}) e^{(1+2\gamma) \int_0^t \|\nabla v(\cdot, s)\|_{L^\infty} ds} + \|\nabla v(\cdot, t)\|_{L^\infty} |\nabla_\alpha X(\cdot, t)|_\gamma.$$

Now integrate (104) and use Gronwall’s lemma to obtain:

$$|\nabla_\alpha X(\cdot, t)|_\gamma \leq C \int_0^t (1 + |\rho_0|_\gamma e^{C_1 s}) e^{(1+2\gamma) \int_0^s \|\nabla v(\cdot, \tau)\|_{L^\infty} d\tau} e^{\int_s^t \|\nabla v(\cdot, \tau)\|_{L^\infty} d\tau} ds. \tag{108}$$

The two desired *a priori* bounds and hence, the conclusion of the proposition follow from (105) and (108). We are left to prove (107). For fluids, an estimate similar to (107) is shown (with vorticity ω in place of density ρ) and the result is presented in lemma 4.8 (chapter 4 [24]). Below we follow similar steps to show (107).

Write the aggregation equation (12a) in the form

$$\rho_t + v \cdot \nabla \rho = -\rho \nabla \cdot v.$$

Hence, using the inverse of the particle-trajectory map, we can re-write it as

$$\rho(x, t) = \rho_0(X^{-1}(x, t)) - \int_0^t \rho \nabla \cdot v(X^{-1}(x, t - s), s) ds.$$

By estimating the Hölder seminorm of ρ , one can show, as in lemma 4.8 [24], that

$$\begin{aligned} |\rho(\cdot, t)|_\gamma &\leq |\rho_0|_\gamma \exp \left[\gamma \int_0^t \|\nabla v(\cdot, s)\|_{L^\infty} ds \right] \\ &\quad + \int_0^t |\rho \nabla \cdot v(\cdot, s)|_\gamma \exp \left[\gamma \int_s^t \|\nabla v(\cdot, s')\|_{L^\infty} ds' \right] ds. \end{aligned} \tag{109}$$

To show the above estimate one has to use the fact that $\nabla_x X^{-1}$ satisfies

$$\|\nabla_x X^{-1}(\cdot, t - s)\|_{L^\infty} \leq \exp \left[\int_s^t \|\nabla v(\cdot, s')\|_{L^\infty} ds' \right].$$

From (19), the calculus inequality (95) and the uniform bound (23) on $\|\rho\|_{L^\infty}$, one can easily derive

$$|\rho \nabla \cdot v(\cdot, s)|_\gamma \leq C_1 |\rho(\cdot, s)|_\gamma. \quad (110)$$

Denote

$$G(t) = |\rho(\cdot, t)|_\gamma \exp \left[-\gamma \int_0^t \|\nabla v(\cdot, s)\|_{L^\infty} ds \right].$$

Multiply (109) by $\exp \left[-\gamma \int_0^t \|\nabla v(\cdot, s)\|_{L^\infty} ds \right]$ and use estimate (110) to obtain

$$G(t) \leq |\rho_0|_\gamma + C_1 \int_0^t G(s) ds.$$

The desired estimate (107) follows from Gronwall's lemma.

References

- [1] Mogilner A and Edelstein-Keshet L 1999 A non-local model for a swarm *J. Math. Biol.* **38** 534–70
- [2] Topaz C M, Bertozzi A L and Lewis M A 2006 A nonlocal continuum model for biological aggregation *Bull. Math. Bio.* **68** 1601–23
- [3] Holm D D and Putkaradze V 2005 Aggregation of finite-size particles with variable mobility *Phys. Rev. Lett.* **95** 226106
- [4] Holm D D and Putkaradze V 2006 Formation of clumps and patches in selfaggregation of finite-size particles *Physica D* **220** 183–96
- [5] Benedetto D, Caglioti E and Pulvirenti M 1997 A kinetic equation for granular media *RAIRO Modél. Math. Anal. Numér.* **31** 615–41
- [6] Toscani G 2000 One-dimensional kinetic models of granular flows *M2AN Math. Model. Numer. Anal.* **34** 1277–91
- [7] Haile J 1992 *Molecular Dynamics Simulation: Elementary Methods* (New York: Wiley)
- [8] Bernoff A J and Topaz C M 2011 A primer of swarm equilibria *SIAM J. Appl. Dyn. Syst.* **10** 212–50
- [9] Bodnar M and Velazquez J J L 2006 An integro-differential equation arising as a limit of individual cell-based models *J. Diff. Eqns* **222** 341–80
- [10] Burger M and Di Francesco M 2008 Large time behavior of nonlocal aggregation models with nonlinear diffusion *Netw. Heterog. Media* **3** 749–85
- [11] Laurent T 2007 Local and global existence for an aggregation equation *Commun. Partial Diff. Eqns* **32** 1941–64
- [12] Bertozzi A L and Laurent T 2007 Finite-time blow-up of solutions of an aggregation equation in \mathbf{R}^n *Commun. Math. Phys.* **274** 717–35
- [13] Bertozzi A L, Laurent T and Rosado J 2011 L^p theory for the multidimensional aggregation equation *Commun. Pure Appl. Math.* **64** 45–83
- [14] Leverentz A J, Topaz C M and Bernoff A J 2009 Asymptotic dynamics of attractive–repulsive swarms *SIAM J. Appl. Dyn. Syst.* **8** 880–908
- [15] Fellner K and Raoul G 2010 Stable stationary states of non-local interaction equations *Math. Models and Methods Appl. Sci. (M3AS)* **20** 2267–91
- [16] Bertozzi A L, Carrillo J A and Laurent T 2009 Blow-up in multidimensional aggregation equations with mildly singular interaction kernels *Nonlinearity* **22** 683–710
- [17] Huang Y and Bertozzi A L 2010 Self-similar blowup solutions to an aggregation equation in \mathbf{R}^n *SIAM J. Appl. Math.* **70** 2582–603
- [18] Topaz C M and Bertozzi A L 2004 Swarming patterns in a two-dimensional kinematic model for biological groups *SIAM J. Appl. Math.* **65** 152–74
- [19] Bodnar M and Velazquez J J L 2005 Derivation of macroscopic equations for individual cell-based models: a formal approach *Math. Methods Appl. Sci.* **28** 1757–79
- [20] D’Orsogna M R, Chuang Y-L, Bertozzi A L and Chayes L S 2006 Self-propelled particles with soft-core interactions: patterns, stability and collapse *Phys. Rev. Lett.* **96** 104302
- [21] Du Q and Zhang P 2003 Existence of weak solutions to some vortex density models *SIAM J. Math. Anal.* **34** 1279–99 (electronic)
- [22] Bertozzi A L, Garnett T and Laurent J B 2011 Characterization of radially symmetric finite time blowup in multidimensional aggregation equations *SIAM J. Math. Anal.* submitted

- [23] Velázquez J J L 2004 Point dynamics in a singular limit of the Keller–Segel model. I. Motion of the concentration regions *SIAM J. Appl. Math.* **64** 1198–223
- [24] Majda A J and Bertozzi A L 2002 Vorticity and incompressible flow (*Cambridge Texts in Applied Mathematics* vol 27) (Cambridge: Cambridge University Press)
- [25] Beale J T, Kato T and Majda A 1984 Remarks on the breakdown of smooth solutions for the 3-D Euler equations *Commun. Math. Phys.* **94** 61–6
- [26] Du Y 2006 Order structure and topological methods in nonlinear partial differential equations (*Series in Partial Differential Equations and Applications* vols 1 and 2) (Hackensack, NJ: World Scientific)
- [27] Eastman S and Estep D 2007 A power method for nonlinear operators *Appl. Anal.* **86** 1303–14
- [28] Kolokolnikov T, Sun H, Uminsky D and Bertozzi A L 2011 Stability of ring patterns arising from two-dimensional particle interactions *Phys. Rev. E* **84** 015203(R)
- [29] Horn R A and Johnson C R 1990 *Matrix Analysis* (Cambridge: Cambridge University Press) corrected reprint of the 1985 original
- [30] Strogatz S H 2000 From Kuramoto to Crawford: exploring the onset of synchronization in populations of coupled oscillators *Physica D* **143** 1–20
- [31] Horstmann D 2003 From 1970 until present: the Keller–Segel model in chemotaxis and its consequences. I *Jahresber. Deutsch. Math.-Verein.* **105** 103–65
- [32] Lukeman Y L R and Edelstein-Keshet L 2010 Inferring individual rules from collective behavior *Proc. Natl Acad. Sci. USA* **107** 12576–580